END

FILMED

DTIC

			1.0		4.5 5.0 5.6 6.3 7.1 8.0	2.8 3.2 3.6 4.0	2.5 2.2 2.0
			1.1				1.8
			1.25		1.4		1.6

MICROCOPY RESOLUTION TEST CHART

NUCLEAR MAGNETIC RESONANCE GYROSCOPE

D. M. Pepper and H. T. M. Wang

Hughes Research Laboratories
3011 Malibu Canyon Road
Malibu, CA 90265

December 1982

FEB 2 8 1983

H
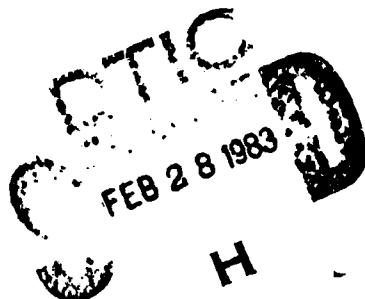
Prepared For
AIR FORCE OFFICE OF SCIENTIFIC RESEARCH
Bolling AFB
Washington, D.C. 20332

UNCLASSIFIED

REPORT DOCUMENTATION PAGE	READ INSTRUCTIONS BEFORE COMPLETING FORM

1. REPORT NUMBER	2. GOVT ACCESSION NO.	3. RECIPIENT'S CATALOG NUMBER
AFOSR-TR- 83-0023	A124 925	

4. TITLE (and Subtitle)	5. TYPE OF REPORT & PERIOD COVERED
NUCLEAR MAGNETIC RESONANCE GYROSCOPE	Final Report 1 Feb. 1980-31 May 1982
	6. PERFORMING ORG. REPORT NUMBER

7. AUTHOR(s)	8. CONTRACT OR GRANT NUMBER(s)
David M. Pepper and Harry T.M. Wang	F49620-80-C-0046

9. PERFORMING ORGANIZATION NAME AND ADDRESS	10. PROGRAM ELEMENT, PROJECT, TASK AREA & WORK UNIT NUMBERS
Hughes Research Laboratories 3011 Malibu Canyon Road Malibu, CA 90265	6110 2F 2301 /A1

11. CONTROLLING OFFICE NAME AND ADDRESS	12. REPORT DATE
Air Force Office of Scientific Research /NP	Dec. 1982
Bolling AFB	13. NUMBER OF PAGES
Washington, DC 20332	74

14. MONITORING AGENCY NAME & ADDRESS(if different from Controlling Office)	15. SECURITY CLASS. (of this report)
	UNCLASSIFIED
	15a. DECLASSIFICATION DOWNGRADING SCHEDULE

16. DISTRIBUTION STATEMENT (of this Report)

This manuscript is submitted for publication with the understanding that the United States Government is authorized to reproduce and distribute reprints for governmental purposes.

Approved for public release; distribution unlimited.

17. DISTRIBUTION STATEMENT (of the abstract entered in Block 20, if different from Report)

19. KEY WORDS (Continue on reverse side if necessary and identify by block number)

Gyroscope, atomic/nuclear magnetism, magnetic resonance, optical pumping, nuclear polarization, noble gases, collision transfer, isotopes

20. ABSTRACT (Continue on reverse side if necessary and identify by block number)

A study of the physics of a nuclear magnetic resonance gyroscope is described. Experimental results in nuclear polarization and relaxation in ^{3}He are obtained using an optical pumping apparatus and a high resolution rf spectroscopic technique. Polarization in the metastable states of the heavy noble gases (^{20,21}Ne, ^{129,131,132}Xe) was observed using a similar optical pumping apparatus. A sensitive detection method based on optical polarization of an excited state transition is

DD FORM 1473 EDITION OF 1 NOV 65 IS OBSOLETE

UNCLASSIFIED

developed and compared with the conventional method of monitoring optical
transmission through the optical pumping cell. A new concept for the
optical pumping of odd-mass-numbered heavy noble gas isotopes to pro-
vide for ground-state nuclear polarization is discussed. Significant
polarization in excited state neon was observed via collisional transfer
from optically pumped helium in a cell filled with a mixture of helium
and neon isotopes. The measured polarization was essentially independent
of the isotopic composition.

PREFACE

This final report describes progress in the development of a
Nuclear Magnetic Resonance Gyroscope, during the period of
1 February 1980 to 31 May 1982 under Contract F49620-80-C-0046,
sponsored by AFOSR. Work on this contract has been performed by
Dr. David M. Pepper, member of the Technical Staff, under the
supervision of Dr. Harry T.M. Wang, Head of the Atomic Clocks
Section, Optical Physics Department, Hughes Research
Laboratories. Technical assistance provided by
Messrs. Ted Calderone, Chuck Fetters, Jack Lewis,
Leonard McNulty, and Joseph Schmid is gratefully acknowledged.
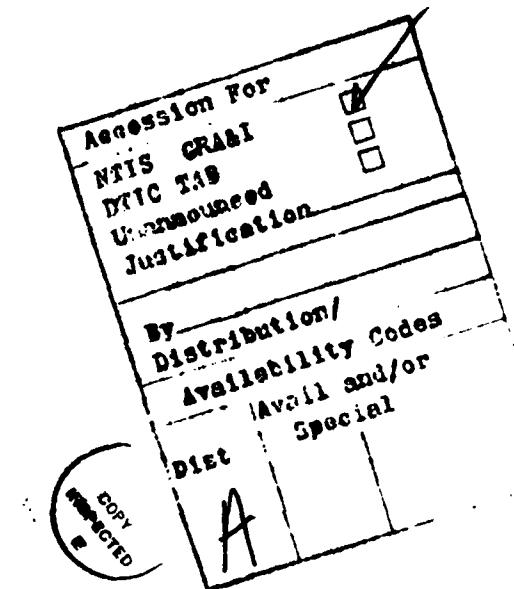
TABLE OF CONTENTS

LIST OF ILLUSTRATIONS

SECTION 1

INTRODUCTION AND SUMMARY

This Final report describes a study on the physics of the nuclear magnetic resonance gyroscope (NMRG) under Contract F49620-80-C-0046, sponsored by AFOSR, during the period 1 February 1980 to 31 May 1982. Technical efforts on this program have further benefited through additional support provided by internal company research funding.

The NMRG is a device that uses magnetic resonance phenomena to measure inertial rotation rates, which can then be integrated to give angular displacement. Nuclear and/or atomic magnetism, which are inherent properties of certain atomic species, are used as the sensing element to replace the rotating mechanical mass or flywheel of the classical gyroscope. The atomic gyro sensor is expected to be compact and reliable, and unlike its mechanical counterpart, there is no bearing to wear out, eliminating periodic recalibration. This reduced maintenance requirement would lead to significant savings in the life cycle cost.

The operation of the NMRG follows from the fact that a magnetic moment precesses about a magnetic field, H_O, in which it is placed. This Larmor precessing frequency, ω_L, is given by

$$\omega_L = \gamma H_O \ ,$$

where the gyromagnetic ratio γ is a characteristic constant of the atomic species. If a system containing the precessing magnetic moment is itself rotating at an angular velocity, ω_r, about the direction of H_O, then the observed precession frequency is shifted to

$$\omega = \gamma H_O - \omega_r \ .$$

Thus, the inertial rotation rat ω_r can be inferred from a precise measurement of the Larmor precession frequency of a given magnetic moment in a known magnetic field H_O. In practice, a

11

magnetic field tends to drift. A closed-loop servo control is required to obtain a certain degree of stability. For this reason, it is necessary to have a second species with a different magnetic moment in the gyro sensor. By observing two magnetic resonances simultaneously in the same magnetic field, the effect of field fluctuations can be eliminated.

Currently, several NMRG designs are under investigation. Each suffers from one or more fundamental problems. These are related to the practice of creating nuclear polarization by optical pumping and observing the nuclear magnetic resonance (NMR) in the same optical pumping cell. Several detrimental effects are incurred by using this approach. First, systematic NMR frequency shifts have been observed. These are caused by real and virtual transitions in the optical pumping cycle[1] or by interatomic collisions (such as spin exchange and metastability exchange collisions[2]) associated with the processes of creating nuclear polarization. Second, such processes also produce line broadening,[1,2] which prevents the full potential of long nuclear relaxation times from being realized. The third problem involves the use of atomic species possessing a nuclear electric quadrupole moment in the presence of alkali or metallic vapors. In one design, nuclear polarization in ground-state noble gas atoms is obtained by collision transfer from optically pumped rubidium vapor, and another employs optically pumped mercury isotopes. In each case, an isotope with a nuclear spin greater than 1/2, and hence possessing a nuclear electricl quadrupole moment, is used in the dual isotope NMRG sensor. The species possessing a quadrupole moment is sensitive to electric-field-gradient-induced relaxation. In this regard, the condensation of metallic vapors on the walls of the optical pumping cell makes the system non-isotropic. Indeed, orientation-dependent nuclear relaxation has been observed.[3] This is unsatisfactory for an inertial rotation sensor.

A gyro sensor that uses optically pumped helium isotopes has also been considered. The reference atomic transitions are

12

provided by the ground state NMR in ^{3}He and a Zeeman transition in metastable ^{4}He. Since the metastable lifetime is limited by wall and/or interatomic collisions, the resultant linewidth can be appreciable, thus limiting the ultimate angular rate resolution of the NMRG sensor.

To overcome the problems encountered in current designs, we have conceived a novel NMRG sensor geometry in which optical pumping and NMR observations are conducted in separate but connected regions, as shown schematically in Figure 1. This novel dual-chamber configuration is referred to as the "dumbbell geometry" (in reference to its characteristic shape) and provides separation that will effectively prevent the systematic frequency shift and line-broadening phenomena in the observed NMR transitions. This geometry was first used successfully in a self-sustained oscillating ^{3}He nuclear Zeeman maser,[4] and has since been utilized by other experimenters[5,6] in subsequent ^{3}He polarization studies.

Using the above geometry, we propose to use two odd-mass-numbered noble gas isotopes as the working materials. Since the ground state of the noble gas atoms possesses a closed electronic
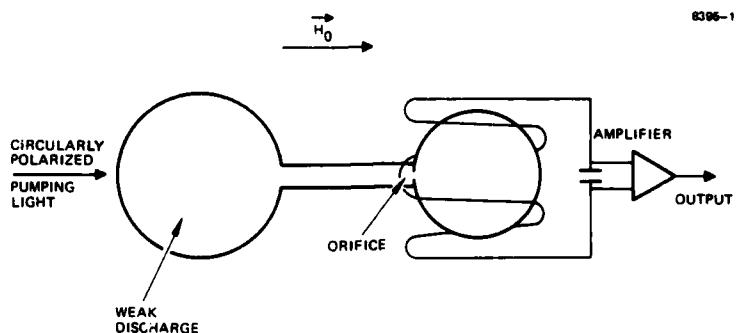
Figure 1. NMR gyro sensor with separated regions for optical pumping and NMR observation.

13

shell configuration, their nuclear moments are effectively shielded from external perturbations, resulting in long nuclear relaxation times (and, therefore, narrow NMR linewidths). This fact enables the polarized ground-state atoms to diffuse from the optical pumping region to the NMR observation region of the dumbbell geometry without appreciable loss of polarization.[4] Furthermore, a system using only noble gas atoms should minimize, if not completely eliminate, the orientation-dependent relaxation phenomenon observed in systems containing a nuclear electric quadrupole moment in the presence of a metallic vapor (as discussed above). Two combinations of noble gas isotopes have been selected for study as possible NMRG sensors.

First, the odd-mass-numbered xenon isotopes ^{129}Xe and ^{131}Xe have been selected as the working matrials because of the advantage of creating nuclear orientation in both isotopes using a common resonant optical pumping lamp. Moreover, the ground-state nuclear relaxation times for these naturally abundant isotopes have been measured to be greater than 20 min.[7]

Second, the dual-isotope combination of ^{3}He and ^{21}Ne has been selected for this study, since ^{3}He, with a ground-state nuclear polarization as high as 40% obtained by optical pumping and a measured nuclear relaxation time of nine days, offers the most desirable attributes for an NMRG sensor. In addition, the low polarizability of neon compared to other heavier noble gases[8] is expected to result in a long nuclear relaxation time. Also, the polarization of ground state ^{21}Ne by optical pumping[9] and of excited states via collisions with optically pumped helium in a ^{4}He-^{20}Ne discharge has been observed.[10] Moreover, the availability of high isotope enrichment (99.9% + for ^{3}He, and 90% for ^{21}Ne) for these isotopes is an additional advantage. Systems using only noble gases will enable rapid warm-up times for potential tactical NMRG device operation.

During this program, we have designed and successfully constructed an experimental apparatus to study magnetic resonances

14

of optically pumped noble gases. Initial efforts have been
directed to the observation of resonances in helium-3 (^{3}He).
Being the least complex noble gas (i.e., a closed s-shell config-
uration), ^{3}He possesses a nuclear spin (I) of 1/2 and has the
smallest polarizability, and hence the longest nuclear
polarization relaxation time of the noble gases. Also, ^{3}He can
be obtained readily with isotopic enrichments in excess of
99.999%, providing extremely pure samples, essentially free of
relaxation-inducing collisions with foreign gases.

After successful system checkout of ^{3}He, efforts were
directed to the study of optical pumping of the heavy noble
gases: Ne and Xe. Based on the result of this study, we then
concentrated our attention on the binary system of ^{3}He and ^{21}Ne.

Highlights of our progress include the following:

- Construction of a multinoble gas ^{3,4}He, ^{NAT,21}Ne, ^{NAT,129,131}Xe

- Fabrication and successful operation of He, Ne, and Xe pump lamps

- Fabrication and successful operation of isotopic- ally enriched He, Ne, and Xe single and binary mixture filled absorption cells

- Fabrication and initial checkout of dual-chamber absorption cells, filled with single and binary mixtures of isotopically enriched noble gases

- Construction of an experimental apparatus (includ- ing magnetic field current source, electronics, pump lamp intensity servo system, optical and rf detection system, and optical components) for studying the various Zeeman resonances

- Observation of ground state ^{3}He (as well as meta- stable and ionic ^{3}He) Zeeman resonances using two different techniques: (1) changes in ^{4}He pump light transmission through a ^{3}He absorption cell; and (2) changes in the optical polarization state of a selected ^{3}He absorption cell fluorescence line

- Observation of the "storage" of ground state, polarized ^{3}He atoms in a dual-chamber absorption cell

15

- Observation of an rf "opto-galvanic" signal caused by metastable ^{3}He absorption of ^{4}He photons (at 1.08 μm). The phenomenon has implications for source stabilization in systems using laser pumps

- Development of the concept of monochromatic optical pumping of selected, isolated two-level transitions of metastable, "heavy," odd-mass numbered, noble gases (e.g., ^{21}Ne, ^{129}Xe, ^{131}Xe)

- Observation of ^{3}P$_2$ metastable Zeeman resonances of heavy noble gases (^{20,21}Ne, ^{129,131,132}Xe) using the respective noble gas pump lamps

- Observation of polarized excited state ^{20,21}Ne atoms, by means of collision transfer from optically pumped ^{3,4}He in a binary (He-Ne) mixture; the large measured polarizatrion (~1%) is essentially independent of the isotopic composition used.

The latter result is significant in that only a <u>single</u> optical pumping source (He) is required to simultaneously pump <u>two</u> different atomic species (He and Ne). As discussed above, since this combination represents the most desirable pair of atoms for a tactical NMRG, this experimental result represents a promising step toward its realization. It is the task of an AFOSR follow-on effort, F49620-82-C-0095, to search for ground-state polarization in this binary gas mixture, using direct rf NMR techniques.

In the next section, we will describe these accomplishments in greater detail, along with typical results.

SECTION 2

PROGRESS AND EXPERIMENTAL RESULTS

In the first part of this section, we will review the basic physics of the optical pumping process for both ^{3}He and the heavy noble gases. This will be followed by a discussion of optical pumping in binary noble gas mixtures. We will then discuss the experimental apparatus that we have fabricated during this program. Subsequent portions will deal with typical experimental results that we have obtained, and conclude with directions for experimental efforts that are being pursued on a continuing AFOSR supported program.

A. OPTICAL PUMPING OF SINGLE NOBLE GAS SPECIES

In this section, we will describe the basic physics that relates to the optical pumping of single, noble gas species. We first address the optical pumping of ^{3}He, the simplest noble gas atom. This will be followed by a discussion of the optical pumping scheme as applied to the heavy noble gases. Even though the heavy noble gases under consideration (Ne, Xe) do not have exactly similar metastable state structures, we will assume that they can be treated under a single category in the present context.

1. Optical Pumping of ^{3}He

The pertinent energy levels for optical pumping of ^{3}He are shown in Figure 2. A schematic of the basic optical pumping apparatus is shown in Figure 3. Metastable 2^3S_1 atoms are created by a weak discharge in a sample of ^{3}He at a pressure of about 1 Torr. The sample thus contains a mixture of ground state and metastable atoms, as well as other discharge products. Typically, the ratio of ground-to-metastable state atom density is approximately 10^6:1. Circularly polarized light at 1.08 µm from a ^{4}He lamp incident collinearly with an externally applied magnetic field will selectively excite the $2^3S_1 \rightarrow 2^3P_0$

17

$5\,^1D$

$\lambda = 4388\text{Å}$

$4\,^1D$

$3\,^1D$

$3\,^3D$

$\lambda = 4923\text{Å}$

$\lambda = 6678\text{Å}$

$\lambda = 5876\text{Å}$

$2\,^1P$

$2\,^3P_0$
1
2

$\lambda = 10,830\text{Å}$

$F = 3/2$: 1.9 MHz/GAUSS; (4 SUBLEVELS)

$2\,^3S_1$

$F = 1/2$: 3.8 MHz/GAUSS; (2 SUBLEVELS)

$1.6 \times 10^5 \text{ cm}^{-1}$

EXCITATION BY
RF DISCHARGE

$1\,^1S_0$

$F = 1/2$: 3.2 kHz/GAUSS; (2 SUBLEVELS)
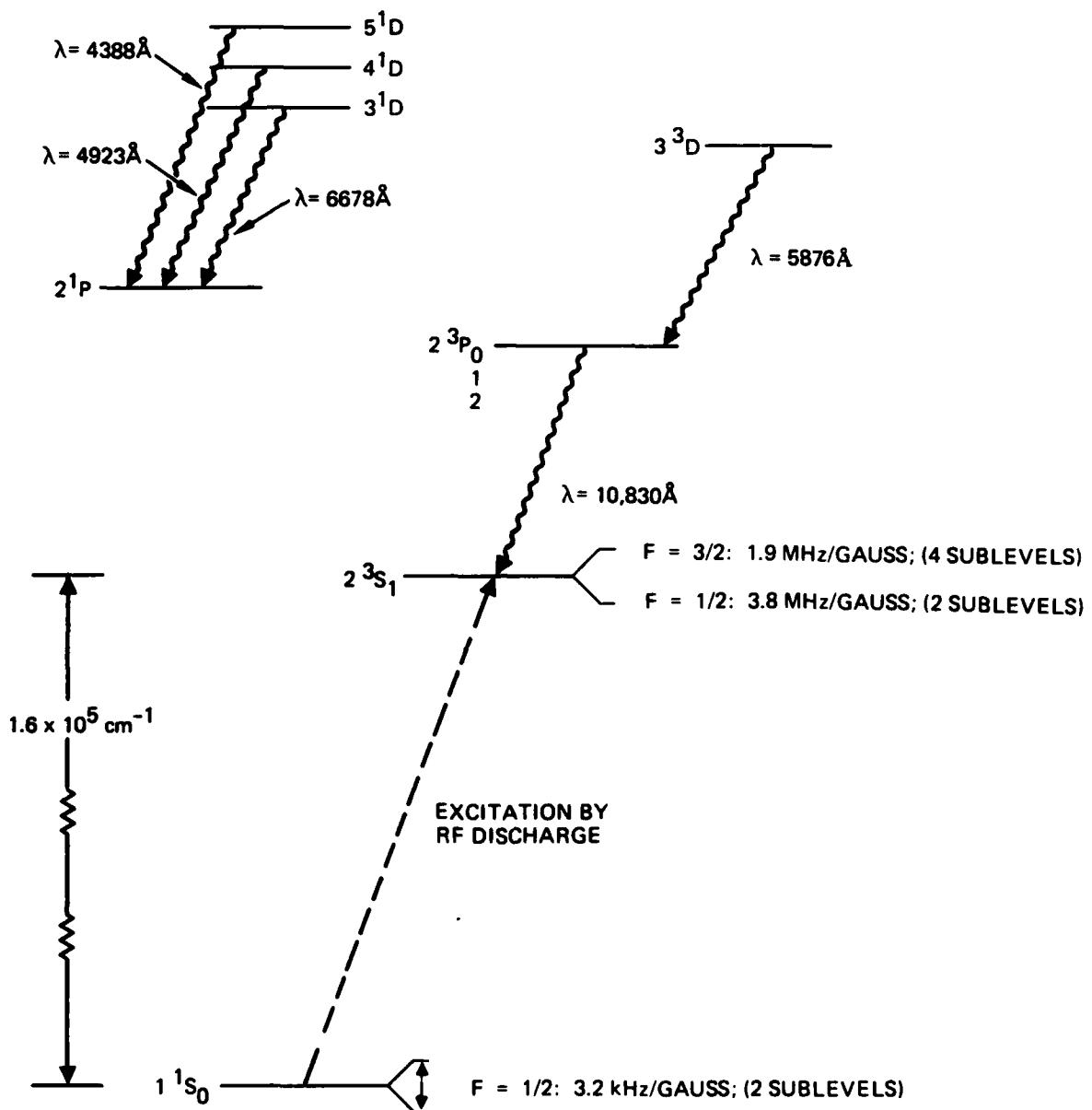
Figure 2.   Energy level diagram pertinent to the optical pumping
of ^{3}He. Also shown are the magnetic-field dependence
of relevant hyperfine sublevels.

18

transition according to the selection rule $\Delta m = +1$ (or -1, depending on the sense of polarization). A ^{4}He lamp is chosen for its favorable isotope shift.[1] Thus, the optically pumped ^{3}He metastables will become polarized (i.e., a population difference of Zeeman sublevels far in excess of the Boltzmann distribution, will result). Metastables in a collision with a neutral atom have a large cross section[11] ($\sim 7 \times 10^{-16}$ cm^2) for the exchange of metastability. Since angular momentum is conserved in such collisions, the metastable polarization is efficiently transferred to the ^{3}He ground state ($1 \, ^1S_0$) nuclear orientation. The tight coupling between the directly pumped metastables and the ground state through metastability exchange results in a large ground-state nuclear polarizaton. Moreover, as a result of the closed s-shell electronic configuration, the nuclear moment is well shielded from external perturbations. Hence, extremely long nuclear relaxation times can be realized under proper conditions, such as by isolating the optical pumping and the NMR observation regions (using the proposed dumbbell geometry).
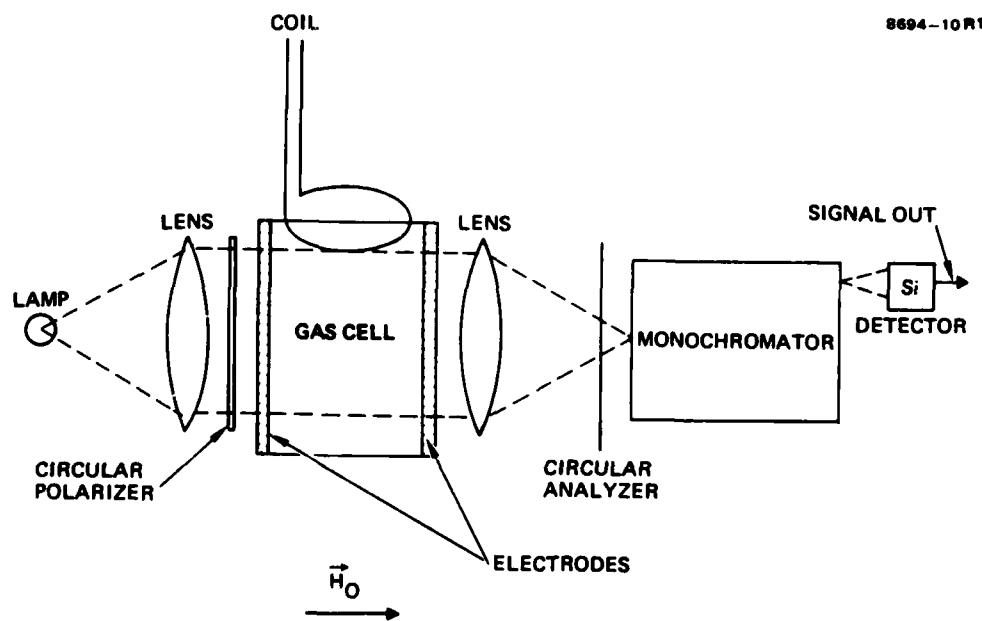
Figure 3. Schematic of an optical pumping apparatus.

The tight coupling between the ground-state nuclear orientation and the metastable polarization enables the ground-state NMR to be conveniently detected by monitoring the changes in transmitted pump light intensity as a test signal is coupled to the absorption cell at the Larmor precession frequency. Alternately, the signal-to-noise (S/N) ratio can be improved by monitoring the optical polarization asymmetry of certain excited state transitions. Since only a specific wavelength is of interest, a narrow bandpass interference filter can be used to suppress the background level. The physical mechanism responsible for this detection scheme is that the ground-state nuclear orientation, which serves as a reservoir of angular momentum, is coupled to the excited states by atomic collision processes. The polarization of the excited state fluoresence is measured by a circular polarization analyzer consisting of a rotating quarter-waveplate (which can be realized either mechanically or electro-optically), followed by a linear polarizer and an optical detector (e.g., a photomultiplier). Examples of excited state transitions in helium that can be used conveniently to monitor ground-state nuclear orientation are the $(2^1P \rightarrow 3^1D)$ and $(2^3P \rightarrow 3^3D)$ transitions at 6,678 Å and 5,876 Å, respectively (see Figure 2). Our apparatus was constructed to monitor the former fluorescence line. Our successful results will be discussed in Section 2-D.

For the dumbbell geometry, separating the optical pumping and the NMR observation regions requires that an rf method similar to the conventional NMR technique be used. In this case, the NMR is detected through changes in the reactance of an rf resonance circuit coupled to the oriented spin when the nuclear Zeeman transition is stimulated. The required rf NMR apparatus is being constructed, and experiments using this scheme are being pursued under an AFOSR-supported follow-on program, which is currently in progress.

2. Optical Pumping of Heavy Noble Gases

As the result of an IR&D program, we have conceived a scheme whereby one may be able to realize large nuclear polarizations in heavy noble gases. The scheme involves the use of a monochromatic optical pumping source to selectively couple an isolated pair of quantum states. Although the energy level structure of the heavy noble gases is similar in nature, we are focusing on the optical pumping of ^{21}Ne for several reasons.

First, it is of interest to verify the viability of the proposed method for optical pumping of heavy noble gases using a monochromatic resonant pumping light. Previous workers[9] have not obtained significant nuclear orientation ($\leq 10^{-5}$) in odd-mass-numbered heavy noble gases (^{21}Ne) by a straightforward extension of the optical pumping technique in ^{3}He. Second, the availability of higher isotope enrichment of about 90% for ^{21}Ne and the relatively small polarizability of neon among heavy noble gases can result in more favorable relaxation times. Third, it may be possible to achieve a (^{3}He-^{21}Ne) dual isotope NMRG sensor. It is evident that ^{3}He has some of the most desirable attributes for use in an NMRG sensor.

An energy level diagram relevant to the optical pumping of neon is shown schematically in Figure 4. The ground-state electronic configuration is a closed shell in the form $2p^6$ $^1S_0$. The first excited state, $2p^5 3s$, consists of four levels: $^3P_{2,1,0}$ and $^1P_1$. The $^3P_{2,0}$ states are metastable, since radiative transition to the ground state is forbidden. It is in these two states that polarization is desired via optical pumping by selective excitation to the $2p^5 3p$ levels (analogous to the case of helium). The $^{3,1}P_1$ states, on the other hand, are radiatively coupled to the ground state. The existence of these two states in the heavy noble gases presents a loss mechanism in terms of the angular momentum transferred to the atoms by absorption of polarized pump photons. (In contrast, for metastable helium, radiative transition to the ground state is strictly forbidden by

21

$np^5 (n + 1)p$ LEVELS

$^3D_3$ $[2p_9]$

OPTICAL
PUMPING
TRANSITION
6402 Å

$^1P_1$

$^3P_0$

$^3P_1$ $[1s_2]$

$^3P_2$ $[1s_3]$ $np^5 (n + 1)s$ LEVELS

$[1s_4]$

$[1s_5]$

RADIATIVE
DECAY (UV)

METASTABILITY
EXCHANGE

$^1S_0$ np^6 GROUND STATE
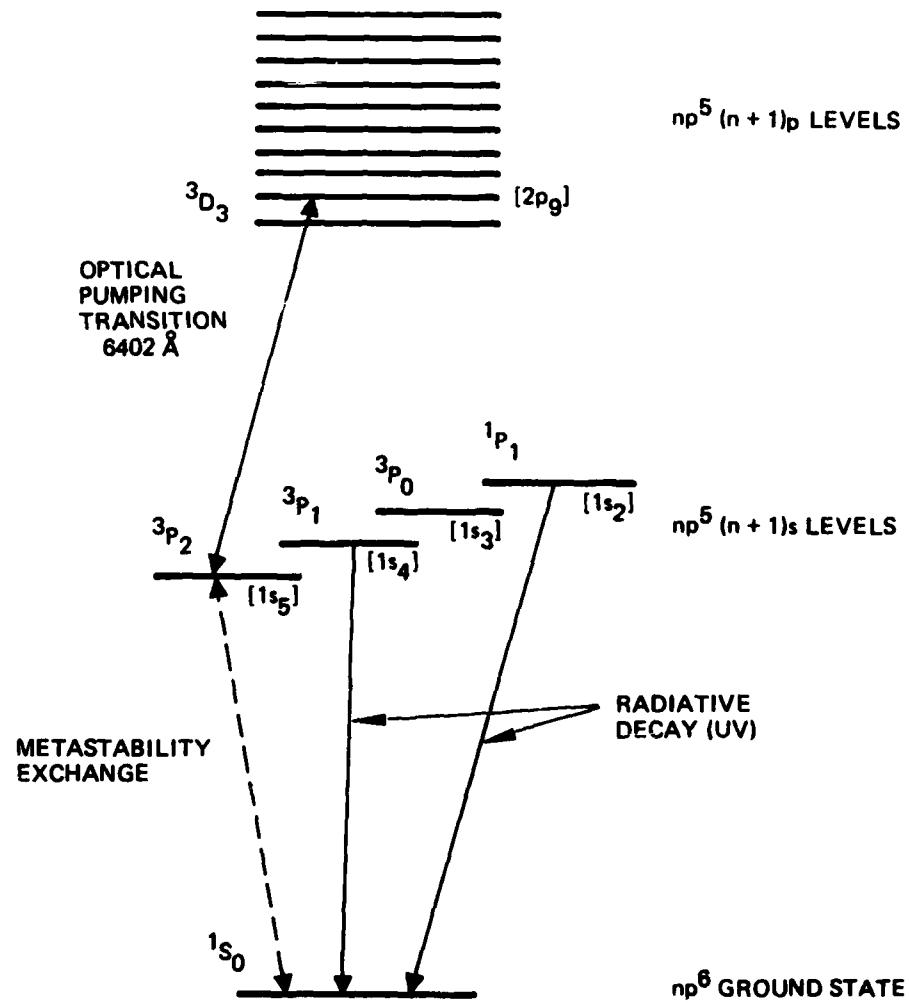
Figure 4. Relevant energy levels in the optical
pumping of heavy noble gases (n = 2 for
neon). [] ≡ Paschen notation.

22

symmetry and parity considerations.) Using an unfiltered
resonant pumping lamp, atoms in the $^3P_{2,0}$ levels can be
transferred to the $^{3,1}P_1$ levels (and hence the ground state) via
transitions to and from the $2p^5 3p$ levels. This population trans-
fer occurs more quickly than the metastability exchange collision
rate. Thus, straightforward extension of the technique of opti-
cal pumping in ^{3}He using an unfiltered resonant pumping lamp is
not expected to give significant ground-state nuclear
orientation.

By using a monochromatic polarized pumping source, this loss
mechansim can be circumvented. In particular, the pump lamp
wavelength will be chosen to correspond to the transition ($3s\,^3P_2$
$\rightarrow 3p\,^3D_3$) at 6,402 Å. Note that the $3p\,^3D_3$ level is not radia-
tively coupled to the other 3s levels. Therefore, the choice of
this transition can be represented as an isolated two-level sys-
tem, similar to that in ^{3}He. Under these conditions, a large
polarization of the metastable $3s\,^3P_2$ level is expected. This
polarization is then transferred to the ground state by metasta-
bility exchange collisions. Indeed, in recent spectroscopic
studies[12] regarding velocity-selective optical pumping processes
in ^{20}Ne, a similar scheme was used to achieve a greater S/N
figure. In the above study, only the metastable state ($^3P_2$) was
probed and, since even isotopes of neon were used, no ground-
state polarization was possible.

Since the other heavy noble gases have similar energy level
structures, this approach should have general applicability if
the proper monochromatic pumping source is selected. For exam-
ple, in the case of xenon, the desired transition ($6s\,^3P_2 \rightarrow 6p\,^3D_3$)
occurs at 8,819 Å. The ultimate attainable ground-state nuclear
orientation will depend on relaxation factors, such as polariza-
bility of the atom, collisional depolarization, and purity of the
isotopic sample.

B. OPTICAL PUMPING OF BINARY NOBLE GAS MIXTURES

We previously selected a mixture of (^{129}Xe, ^{131}Xe) isotopes as working materials for a dual-isotope NMRG sensor. The selection was based on the expectation that ground-state nuclear polarization can be created in both isotopes using a common resonant pumping source. This would lead to a compact device, which is desirable in real applications. On the other hand, the relatively large depolarization cross section for metastable xenon,[13]

$$\sigma(Xe^m - Xe) = 190 \times 10^{-16} \text{ cm}^2 \quad ,$$

compares rather unfavorably with that for metastable neon in a cell using helium as a buffer gas[10]:

$$\sigma(Ne^m - Ne) = 16.6 \times 10^{-16} \text{ cm}^2$$

$$\sigma(Ne^m - He) = 0.43 \times 10^{-16} \text{ cm}^2 \quad .$$

The smaller neon metastable depolarization cross section is caused by the smaller polarizability of neon compared to the heavier noble gases.[8] Moreover, the best isotopic enrichment for the odd-mass-numbered xenon isotopes is only about 60%, while ^{21}Ne is available with a purity of 90%.

The potential for a larger ground-state nuclear orientation and a smaller resonance linewidth for ^{21}Ne compared to the xenon isotopes makes it worthwhile to consider its feasibility for NMRG applications. Specifically, the combination of ^{3}He and ^{21}Ne, for reasons stated earlier, form a favorable pair of working atomic species. At first, one may conclude that because of the different transitions necessary to simultaneously optically pump both species (1.08 μm and 6,402 Å for ^{3}He and ^{21}Ne, respectively), two pump lamps are required. A schematic of such a typical scheme is shown in Figure 5. The linear three-sphere geometry retains the concept of separated regions of optical pumping (for each isotope) and NMR observation. The added components may constitute

24

$\vec{H}_o$

LHCP
^{4}He PUMP
LIGHT

P λ/4

WEAK RF
DISCHARGE

AMP → OUTPUT

RHCP
Ne PUMP
LIGHT

λ/4 P

WEAK RF
DISCHARGE
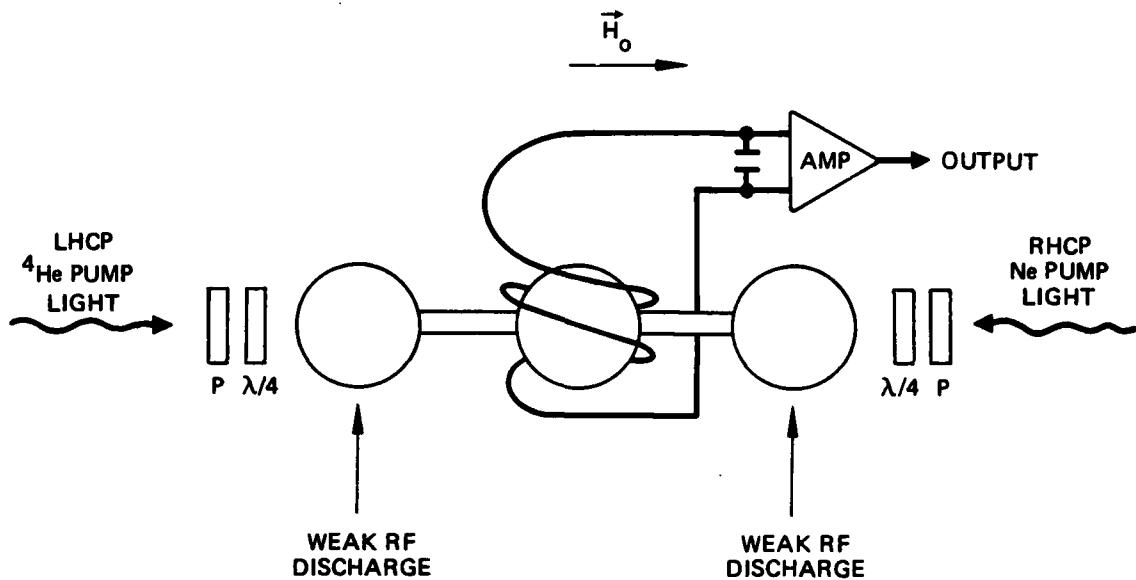
Figure 5.   Linear, three-sphere, dual-isotope NMR gyro sensor
using separate regions for optical pumping of each
isotope and NMR observation.

disadvantages (e.g., size, weight, energy requirements, cost) for
NMRG applications.

Possible solutions to these disadvantages in the He-Ne sys-
tem can be realized upon examination of the energy dynamics in
He-Ne collisions. The existence of near-resonant energy levels
between metastable helium and excited-state neon atoms, as shown
in Figure 6, and by the operation of the He-Ne laser provides a
possible mechanism for collision transfer. The polarization of
excited levels of neon by collisions with optically pumped helium
in an absorption cell has been observed, and in addition, it was
shown that the polarization is retained in lower lying neon
levels by cascaded radiative transitions.[10] Since the experiment
used optical detection techniques involving fluorescence from
excited states of neon, the polarization of the $3s\,^3P_{2,0}$
metastable states was not measured. Moreover, because of the
large percentage of even isotopes in naturally abundant He and
Ne, no ground-state polarization was expected.

25
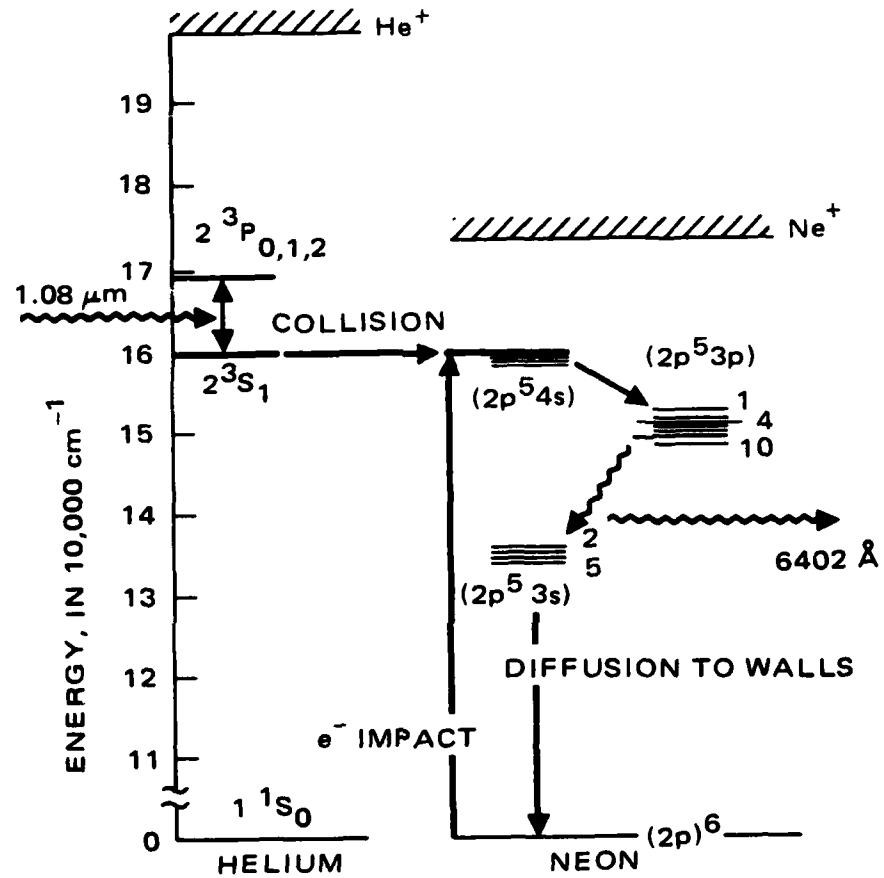
Figure 6. Relevant energy levels in a Ne-Ne system.

In Section D-2, we will describe successful experimental results where significant excited state polarization in both ^{3}He and ^{21}Ne was observed using a single pump lamp (1.08 μm from ^{4}He). The polarization in ^{21}Ne was a factor of five greater than that obtained using direct optical pumping techniques (i.e., 6,402 Å from a Ne pump lamp). In addition, the degree of polarization, within experimental error, was the same in neon, regardless of the isotopic composition of the ^{3,4}He-^{20,21}Ne mixtures. Polarization of ground-state ^{3}He was also maintained even in the presence of the neon species. Furthermore, the excellent S/N ratio observed in metastable ^{21}Ne resonance leads us to expect that significant metastable ^{21}Ne polarization is present. Hence, one anticipates that significant ^{21}Ne ground-state nuclear orientation can be obtained by metastability exchange collisions. This approach could result in a high performance, dual-isotope, all-noble-gas NMRG sensor (using only a single ^{4}He pump lamp), since the desirable features of ^{3}He for NMRG applications are well established. A task in a follow-on AFOSR-supported program currently in progress addresses the experimental verification that simultaneous polarization in ground-state ^{3}He and ^{21}Ne can be observed in a dual-chamber absorption cell.

C.   EXPERIMENTAL APPARATUS AND MEASUREMENT TECHNIQUES

In this section, we will describe the optical pumping apparatus we have fabricated, and discuss the techniques we used to observe the various resonances. Included are details regarding pump lamp and absorption cell fabrication, magnetic field apparatus, and the optical elements (filters, polarizers, detectors, etc.) used. The section concludes with a brief description of the two basic experimental configurations and measurement techniques employed in our studies.

1. Preparation Techniques for Cells and Lamps

Cell preparation techniques are important because the depolarization cross section for impurity contaminants is on the order of gas kinetic. Thus, to optimize ground-state nuclear orientation in noble gases, optical pumping cells must be prepared and maintained at extremely high purity. For this reason, we have designed and fabricated a fill-station and gas-handling system using only stainless steel and glass components. The system is capable of handling seven gases at a time. The cell geometry and filling procedure are designed to achieve the same objective.

For the initial experiments with helium, several Pyrex pump lamps (with ^{4}He fill pressures of 1 to 3 Torr) and absorption cells (with ^{3}He fill pressures of 100, 200, and 900 μm) were constructed. Some of the lamps and cells had separate ballasts connected to the respective lamp (or cell) by means of a capillary tube. Figure 7 is a sketch of a typical cell. The lamps (cells) were baked under high vacuum for several hours;

11069-5

ABSORPTION REGION

PUMPING LIGHT

CAPILLARY TUBE

BALLAST/RESERVOIR

NON-MAGNETIC (BARIUM) EXOTHERMIC GETTER
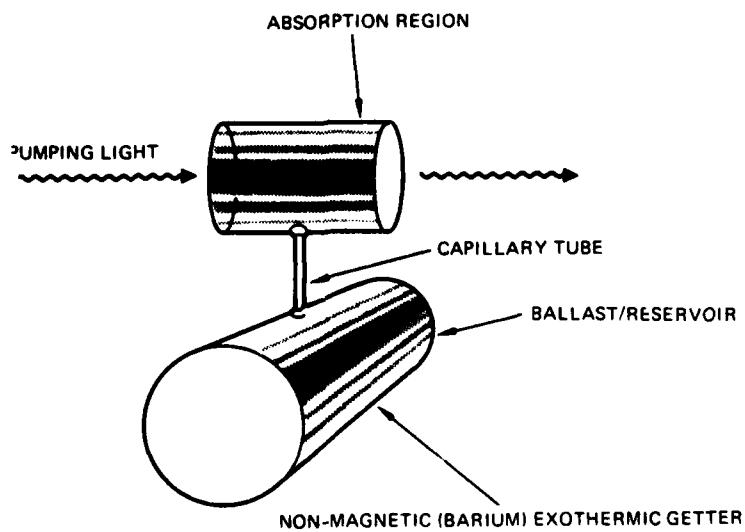
Figure 7. Sketch of a typical absorption cell (or pump lamp).

28

further cleaning was provided by an rf discharge. Typical vacuum pressures in the 10^{-6} to 10^{-9} Torr range were obtained using this technique. Prior to filling with the desired isotope, an exothermic barium (nonmagnetic) getter was flashed to coat the inner surface of the ballast. The getter would pump non-noble gas impurities that might be generated during cell (lamp) operation, with the glass capillary tube providing a diffusion path to the cell (lamp) proper. Observation of NMR signals in ^{3}He indicates the soundness of the procedure.

Absorption cells were also fabricated without the reservoir and getter section. These cells were used for comparative purposes relative to the above geometry. In addition, several absorption cells using ^{3}He were fabricated (for a system checkout) using the dumbbell geometry (shown in Figure 1). The connecting capillary tube (between the pumping and observation region) was 5 cm long, with a 1 cm i.d. bore. To achieve reasonable, geometrical storage times of polarized, ground-state atoms in the observation region, a small aperture was placed within the capillary tube. The apertures were in the 0.5 mm to 2 mm i.d. range, resulting in predicted storage times in the range of ~10 to ~1/2 sec. The apertures were fabricated by inserting a 2 mm long section of a miniature capillary tube (having the small i.d.) within the connecting tube. A glass-to-glass vacuum ring seal was then formed to secure the glass "disk" to the structure.

We have also fabricated Pyrex cells for use in optical pumping experiments using isotopically enriched (as well as naturally abundant) heavy noble gases: neon and xenon. The basic design of the cells (i.e., configuration, getter, etc.) is similar to that of the helium cells and lamps where successful polarization experiments were conducted. We have fabricated both single as well as dumbbell configurations for the absorption cells; the latter geometry provides separate regions for optical pumping and the observation of the NMR signal. The pump lamps contained about 2 to 6 Torr of high purity neon or xenon.

For neon, absorption cells were fabricated containing natur-
ally abundant neon, or 90% isotopically enriched ^{21}Ne(in the 2 to
50 μm Hg range), with or without a buffer gas (^{4}He or ^{3}He, in the
100 to 500 μm Hg range). For the xenon experiments, cells were
constructed containing naturally abundant Xe, or 60% isotopically
enriched ^{129}Xe or ^{131}Xe (in the 2 to 50 μm Hg range), with or
without helium buffer gas. The buffer gas was used to help stab-
ilize the weak rf discharge necessary to produce metastable neon
or xenon atoms. The ratio of partial pressures of He:Ne or He:Xe
was chosen to be less than their respective polarization destruc-
tive cross sections. We note that helium is the optimum buffer
gas, since it possesses the smallest polarization destruction
cross section of all the noble gases. Finally, the use of He as
a buffer gas enabled us to investigate the properties of
collision-induced polarization transfer from optically pumped He
to various excited states of neon.

2. Optical Pumping Apparatus

The optical pumping apparatus is shown schematically in
Figure 8. The initial experiments were conducted with ^{3}He, but
the apparatus is easily modified for use with other noble gas
isotopes (by changing polarizers, filters, waveplates, and/or
detectors). The absorption cell is placed at the center of a
solenoid, which is equipped with a second-order correction coil
to provide a more homogeneous magnetic field. Both the main
solenoid and the correction coil are driven by electronically
adjustable, stabilized current sources (with a stability of about
1 part in 10^6). For our experiments the magnetic field was
adjustable from ~1/2 to ~15 gauss. Surrounding the solenoid is a
set of three concentric cylindrical molypermalloy magnetic
shields which are equipped with flat end-caps to minimize the
effect of ambient field fluctuations. To optimize the shield
performance, degaussing was done using a 60-cycle current by a
technique developed for our hydrogen maser atomic clock, which
was developed under a program in support of the NAVSTAR Global

10366-5R2
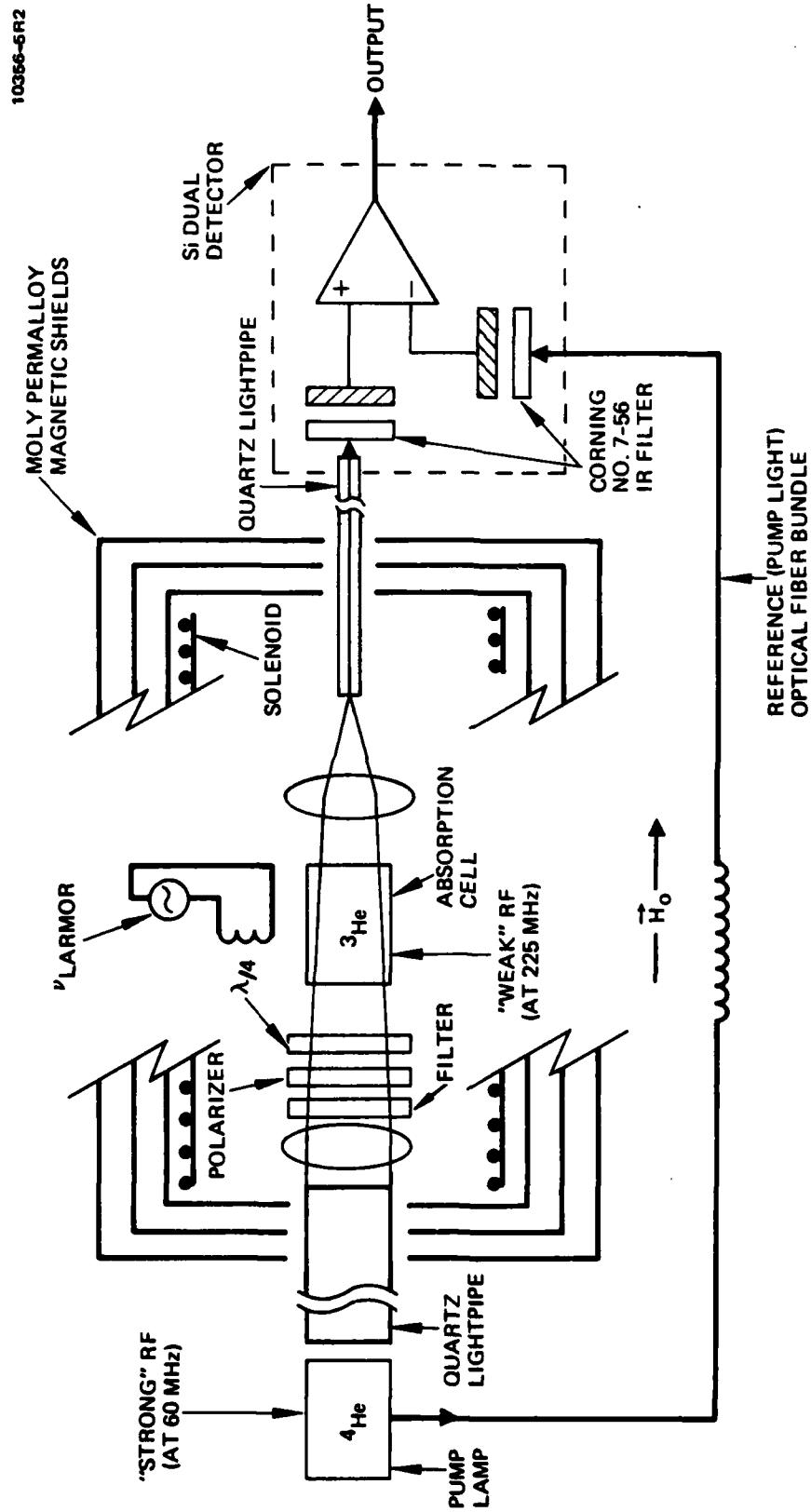
Figure 8. Experimental apparatus. This scheme utilizes pump light transmission changes (through the absorption cell) to detect the various resonances.

31

Positioning System. The pump lamp and the detector are located outside the magnetic shields. Quartz light pipes are used to couple the pump light to the absorption cell and the transmitted light to the detector. This arrangement improved the rf, thermal and magnetic isolation of the components.

The ^{4}He pump lamp is (strongly) excited by an rf power oscillator (P $\sim$ 50 W, ν $\sim$ 60 MHz), which is inductively coupled to the lamp. The 1.08 μm radiation incident upon the ^{3}He absorption cell was measured to be $\sim$1 mW. To produce a population of metastable ^{3}He atoms, the absorption cell was (weakly) driven by a second power oscillator (P $\sim$ 200 mW, ν $\sim$ 200 MHz), which is capacitively coupled by several loops of No. 20 wire surrounding the cell. The homogeneity and uniformity of this resulting ^{3}He discharge is critical in obtaining a large nuclear polarization. Time-varying fields at the Larmor frequencies of the ground-state ^{3}He atom ($\sim$3.2 kHz/G) and of the metastable states ($\sim$1.9 MHz/G and 3.8 MHz/G) were applied to the ^{3}He cell by two separate rf generators, and coupled by two different sets of coils that surrounded the cell. The coils are oriented so that the resultant time-varying magnetic fields are perpendicular to the quantization axis (i.e., the axis containing the static field and the propagation vector of the pump light). We checked to ensure that these two rf sources did not systematically affect the existing ^{3}He cell discharge condition.

The 1.08 μm ^{4}He pumping light is rendered circularly polarized by a Polaroid type HR linear polarizer and an adjustable quarter-wave plate. Proper alignment of the optical axes of the retardation plate resulted in a measured circularity of about 96%. A Kodak type 87C filter is used to pass only the IR line from the pump lamp.

The intensity stability of the pump lamp flux is crucial both for maintaining a constant source of photon angular momentum and for maximizing the S/N ratio when monitoring the optically pumped resonances (using the pump light transmission technique (to be discussed below). Indeed, it has been

experimentally verified[14] that pump light fluctuations can degrade the achievable atomic polarization. It is for these reasons that we designed and fabricated a servosystem that minimizes pump lamp intensity fluctuations and/or drifts. The system operates by monitoring the pump lamp optical output and servoing this signal back into the rf drive unit via an optical fiber bundle. Figure 9 shows performance results using this approach, where the pump lamp output is plotted as a function of time. As can be seen from the figure, the unstabilized pump lamp output not only fluctuates in time, but also drifts. These intensity changes are not only on the same order as the transmission changes that characterize the various resonances (see below), they also occur on the same time scale as the resonances (given the dc field sweep rate). Both of these drawbacks are alleviated with the servoloop in operation: the fluctuations as well as the overall intensity drifts are reduced by at least a factor of 20.

3. Measurement Techniques

There are two techniques that we used to detect the polarization state of the atoms and the various magnetic resonances. The first technique involves monitoring changes in the transmission of the 1.08 μm pump light through the absorption cell as a result of the application of time-varying fields at the Larmor frequencies. The second approach involves observing corresponding changes in the optical polarization state of an isolated ^{3}He fluorescence line, and is referred to as the optical polarization asymmetry (OPA) technique.

The apparatus used for the pump light transmission technique is shown in Figure 8. The resonances are monitored through changes in the intensity of the transmitted pumping light by a compensated silicon detector. An IR filter (Corning No. 7-56) is used to suppress background visible radiation, while the

33
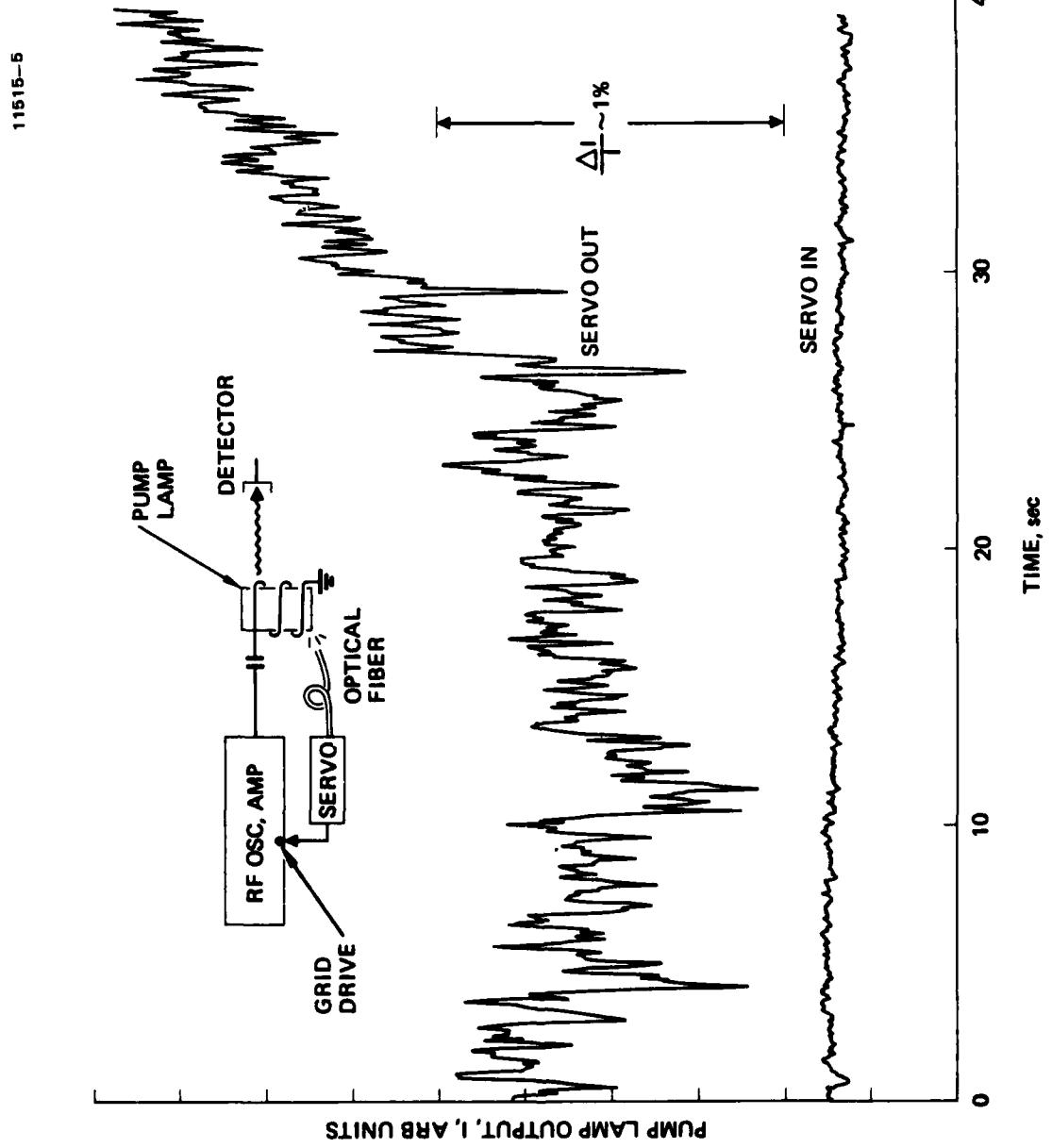
Figure 9. Pump lamp servo characteristics.

34

compensation minimizes the effect of variations in pumping lamp intensity. The compensating signal is derived from the output of a second silicon detector coupled to the pump lamp through an optical fiber bundle. The effectiveness of the technique is underscored by the fact that variations in the transmitted light intensity due to the magnetic resonance are only about 10% of the absolute absorption. Depending on the discharge condition in the absorption cell, the total absorption is just a few percent of the incident pumping light. From the observed S/N, the compensated detector has an effective sensitivity in excess of 1 part in 10^5. The compensated detector scheme and/or the servo system mentioned above were used interchangeably, depending on the detector (or detection technique) utilized.

The polarization of a given set of Zeeman sublevels is determined by the ratio $\delta\alpha/\alpha$, where α is the steady-state metastable absorption of the pump light through the absorption cell, and $\delta\alpha$ is the incremental change in the absorption upon application of the (saturating) Larmor test signal. For ^{3}He, α ranged from 3 to 14%, and $\delta\alpha$ was typically ~1/2%.

The second technique, which can yield a higher S/N ratio than the transmission method, was developed from our assumption that the nuclear polarizations obtainable in the heavy noble gases would be smaller than that in ^{3}He. The experimental geometry is indicated in Figure 10. The basic optical pumping apparatus is similar to that of the transmission technique. However, in contrast to monitoring the transmission of the ^{4}He pump light, the resonances are detected by observing changes in the optical circular polarization state of a selected higher-lying (^{3}He) absorption cell fluorescence line. This technique is made possible by the strong coupling of the ground-state nuclear polarization to the higher lying states by means of angular momentum conserving collisions. In the case of ^{3}He, we have chosen to monitor the (3^1D $\rightarrow$ 2^1P) transition at 6,678 Å. The scheme involves the use of a rotating quarter-wave plate, analyzer, narrow bandpass filter, optical detector (an S-20 photomultiplier tube), and a synchronous detector (i.e., a lock-in amplifier).

35
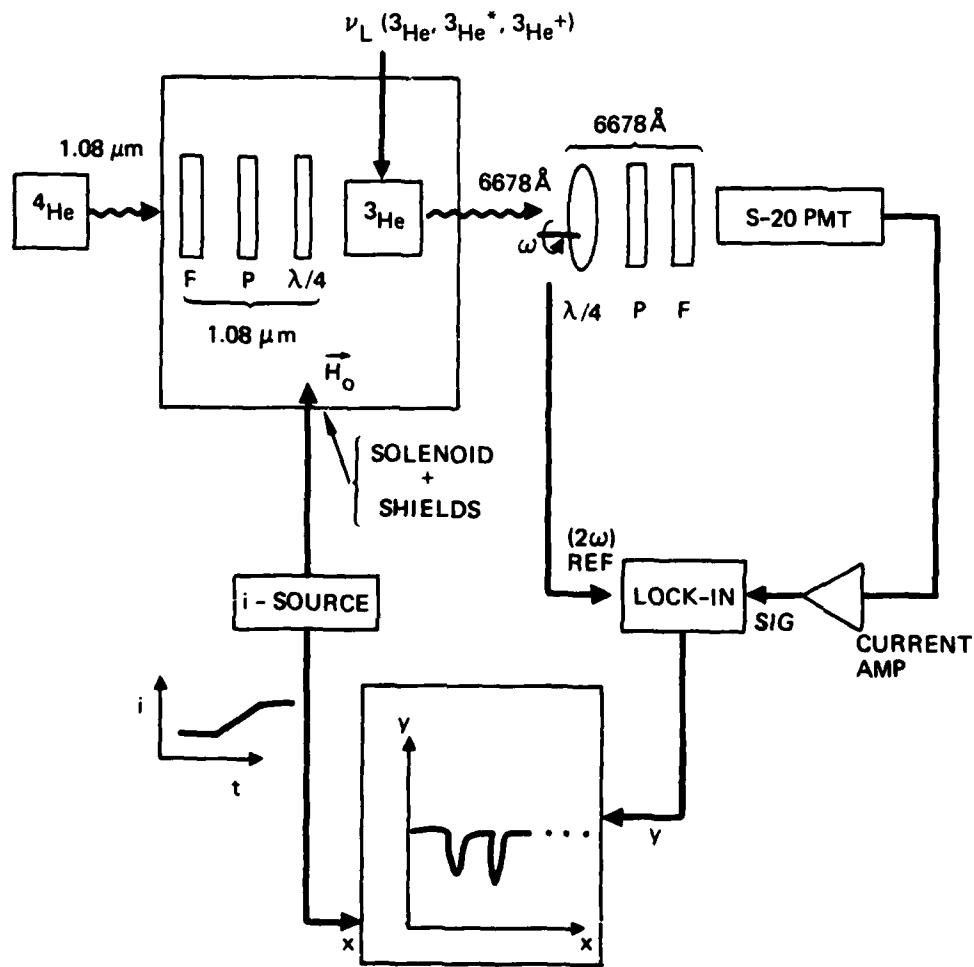
Figure 10.   Experimental apparatus used for the observation
of magnetic resonances via the optical polari-
zation asymmetry of a ^{3}He fluorescence line.

Assuming circularly polarized light incident upon this apparatus, the rotating wave-plate/analyzer pair will yield an amplitude modulated signal at a frequency equal to twice the rotational rate of the wave plate. In our apparatus, the waveplate was rotated at a 10 Hz rate; hence a 20 Hz modulation signal was detected. A HeNe laser beam passing through the same rotating wave-plate was detected and used as the reference input to the synchronous detector. A narrowband dielectric filter (at 6,678 Å) was used to isolate the ^{3}He fluorescence line. No signal was present when either the ^{3}He cell or the pump lamp discharge was extinguished; this ensured the absence of systematic noise sources.

The Zeeman sublevel polarization as measured by the OPA technique was determined by the relative degree of circular polarization of the isolated fluorescence line. This was accomplished by first inserting a circular polarizer between the ^{3}He cell and the rotating waveplate (see Figure 10), without optical pumping (i.e., no pump lamp illumination). The resultant lock-in amplifier output level (corrected for the transmission coefficient of the circular polarizer) thus established a calibrated 100% OPA polarization reference. The fraction of this reference level, as measured under optical pumping conditions, was interpreted as the degree of polarization of the sample.

The linearity of both detection schemes was ensured prior to our measurements through the insertion of various ND filters and/or waveplates.

D.   EXPERIMENTAL MEASUREMENTS AND RESULTS

In this section, we will discuss the key experimental results obtained during this program. The first subsection deals with optical pumping experiments using single noble gas species: He, Xe, and Ne. The second subsection discusses results obtained using binary noble gas mixtures of He and Ne. The positive results obtained using binary gas mixtures constitute a promising step toward the realization of a compact, dual-isotope NMRG sensor.

37

1. Optical Pumping of Single Noble Gas Species

a. Helium

Using ^{3}He as the optically pumped species, we have observed metastable absorption of 1.08 μm pump light from a ^{4}He lamp, leading to significant metastable and ground-state polarization (~9.5%). Both of the optical detection techniques described above were successfully utilized, with the OPA approach permitting us to observe Zeeman resonances in the ionic ground state of ^{3}He, as well as evidence of the "storage" of ground-state polarized ^{3}He atoms in the ballast section of an absorption cell. Finally, we have observed an rf analog to the optogalvanic effect; this scheme can be of use in frequency stabilizing an optical source (e.g., a diode or color center laser) to the 1.08 μm ^{3}He absorption line.

(1) **Pump Light Transmission Technique** — Our measurements began with a determination of the metastable density in the absorption cell. The cell was filled with ^{3}He to 900 μm. The measured absorption of the pump light over the 5 cm length of the cell as a function of the rf power that drives the ^{3}He absorption cell discharge is shown in Figure 11. The absorption varied from 3 to 14%, corresponding to a deduced metastable density of 3 to 14×10^9 cm^{-3}. For stable discharge operation, and to minimize discharge-induced relaxation, the following measurements were made at a discharge level corresponding to a 4% ^{3}He metastable absorption.

The incident pump lamp power at the front window of the absorption cell was about 1 mW. This modest pump lamp intensity resulted in an optical pumping time (i.e., time to establish equilibrium ground-state nuclear polarization) of about 30 sec, as shown in Figure 12. The NMR signal was monitored by optical transmission using the scheme shown in Figure 8. After equilibrium was established, as indicated by a steady transmission of the pumping light, the NMR test signal frequency was quickly swept across resonance. The destruction of nuclear polarization decreased the pump light transmission; it took the indicated pumping time for transmission to recover. The strength of the
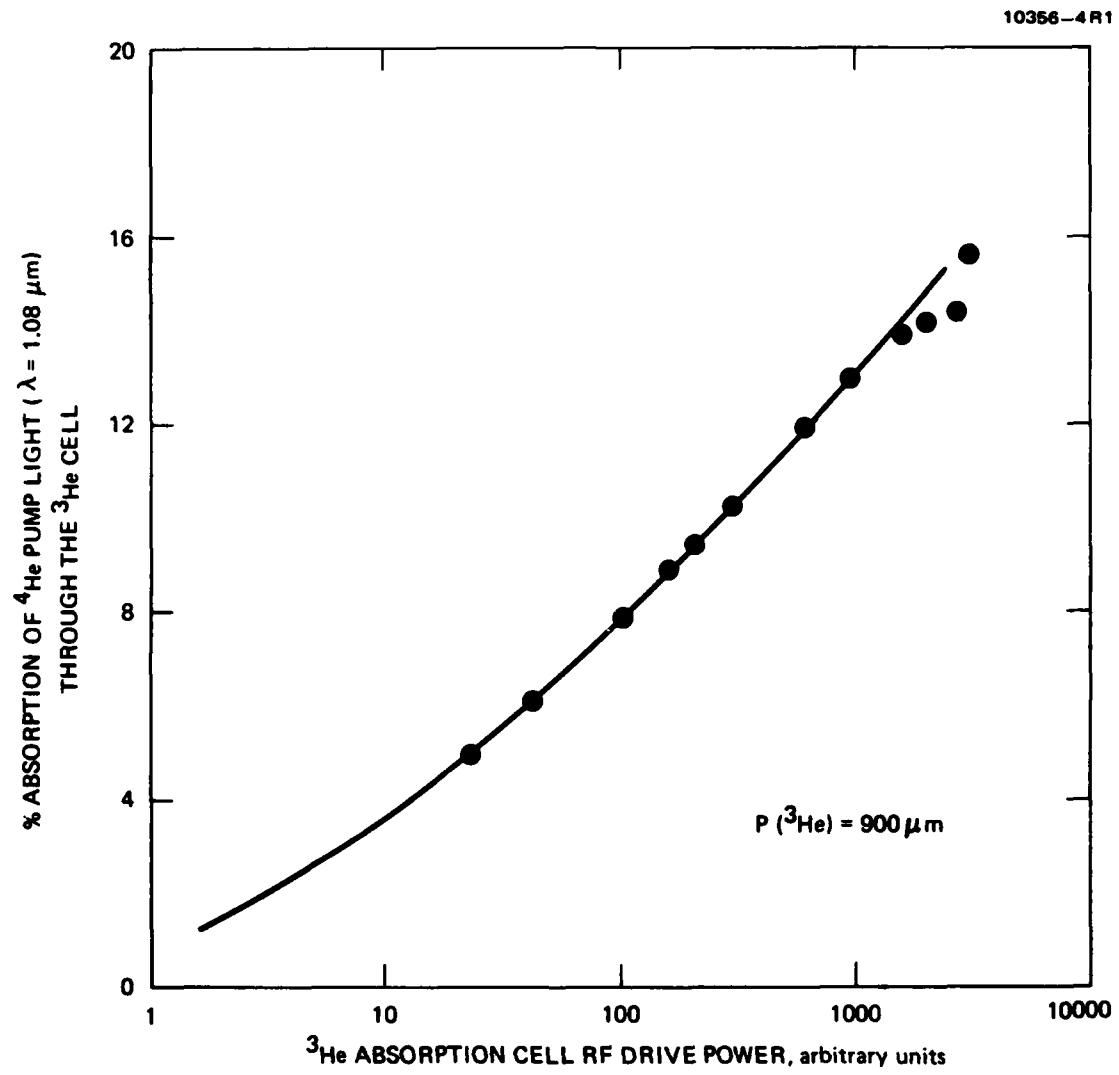
Figure 11. Measured ^{3}He metastable (^{3}He*) absorption of the ^{4}He pump light (at 1.08 µm), over a 5 cm path length, as a function of absorption cell drive power (measured in terms of the ^{3}He flourescence). The lowest absorption yields a ^{3}He* density of ~4 x 10^9 cm^{-3}. The total ^{3}He density is ~3.2 x 10^{16} cm^{-3}; P(^{3}He) = 900 µm.
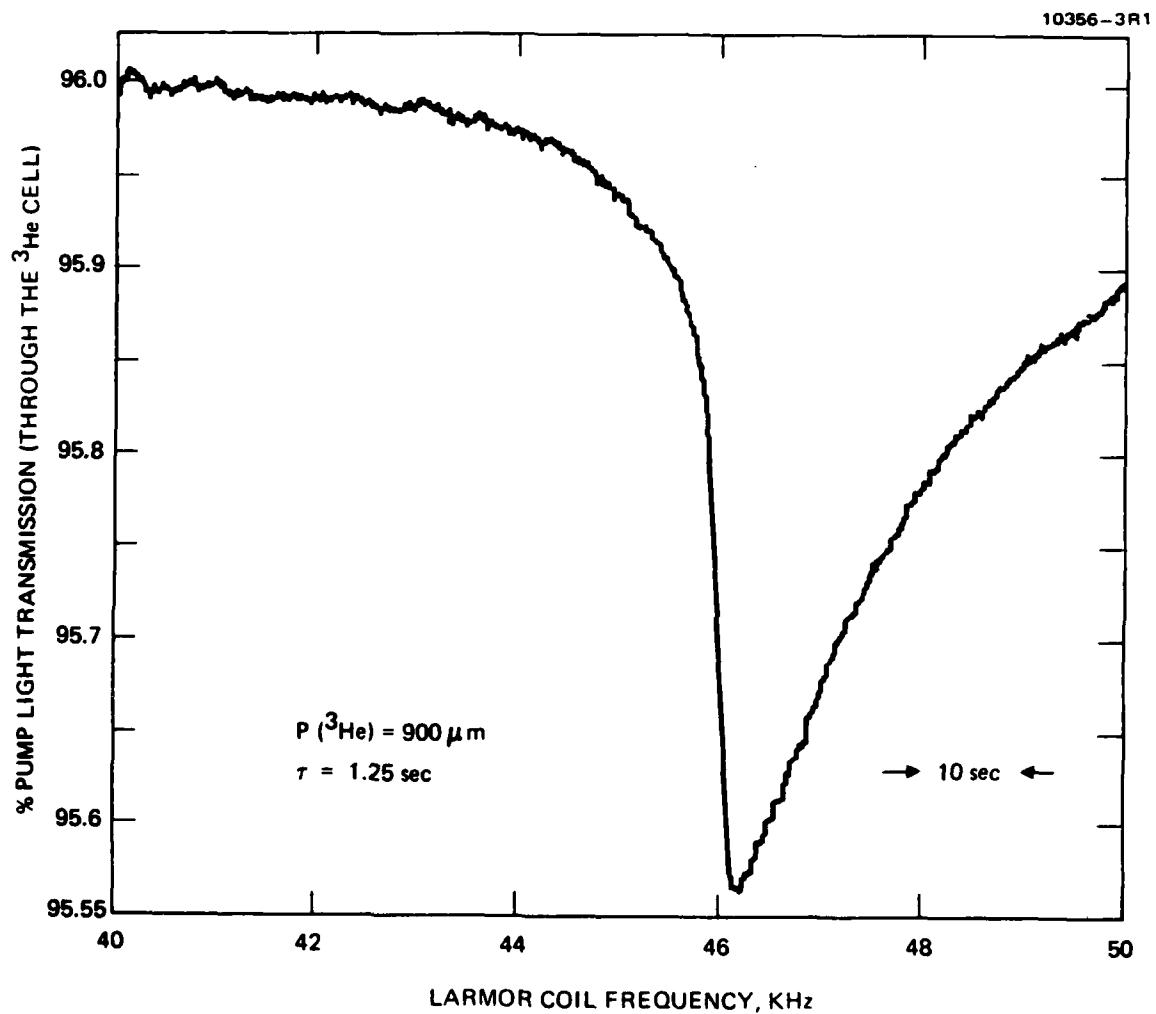
Figure 12. Measurement of the ^{3}He optical pumping time from observation of the NMR signal. The frequency sweep rate is ~0.1 kHz/sec.

40

signal at resonance implies a nuclear polarization of about 4.6%. Since this result, we have improved our apparatus (i.e., the ^{3}He discharge conditions) with a measured nuclear polarization of 9.5%.

Another trace of the NMR signal using pulse modulation and synchronous detection is shown in Figure 13. The Larmor frequency pulse repetition rate was about 3 Hz, with a duty cycle of about 15%. The RC time constant of the synchronous detector was 1.25 sec. The 300 Hz linewidth is a result of several fctors, including rf power broadening, collision with other discharge products, and magnetic field gradients. The disparity between the expected relaxation time of about 0.1 sec in the conventional absorption cell and the optical pumping time of 30 sec makes it difficult to measure the true linewidth by the optical detection method without drastic rf power broadening. However, by using the dumbbell geometry and rf detection techniques (for which hardware is currently being fabricated) we can circumvent this problem.

Another relevant parameter measured — the variation of the nuclear polarization with the ^{3}He cell absorption coefficient — is shown in Figure 14. The result is consistent with the expectation that in the limit of a weak discharge the production of metastables is so small that the net pump photon coupling rate is inadequate. Conversely, in the limit of a strong discharge, discharge-product-induced relaxation will dominate, resulting in a lower polarization.

In another set of experimental runs, the changes in pump light transmission were monitored by fixing the test oscillator freuency, while slowly scanning the applied magnetic field. This enables us to optimize the coupling of the (Larmor) rf coils to the ^{3}He atoms by using tuned circuits. The coil was driven at ~5.7 kHz for the ground-state NMR. In addition, a second coil, driven at 12.28 MHz, was placed around the absorption cell to couple to several other ^{3}He resonances: the two ^{3}He $2\,^3S_1$ metastable Zeeman resonances at 1.9 MHz/G and at 3.8 MHz/G

LARMOR COIL FREQUENCY

10366-2R1

← 1 kHz →

P (^{3}He) = 900 μm

PUMP LIGHT TRANSMISSION (THROUGH THE ^{3}He CELL), ARBITRARY UNITS
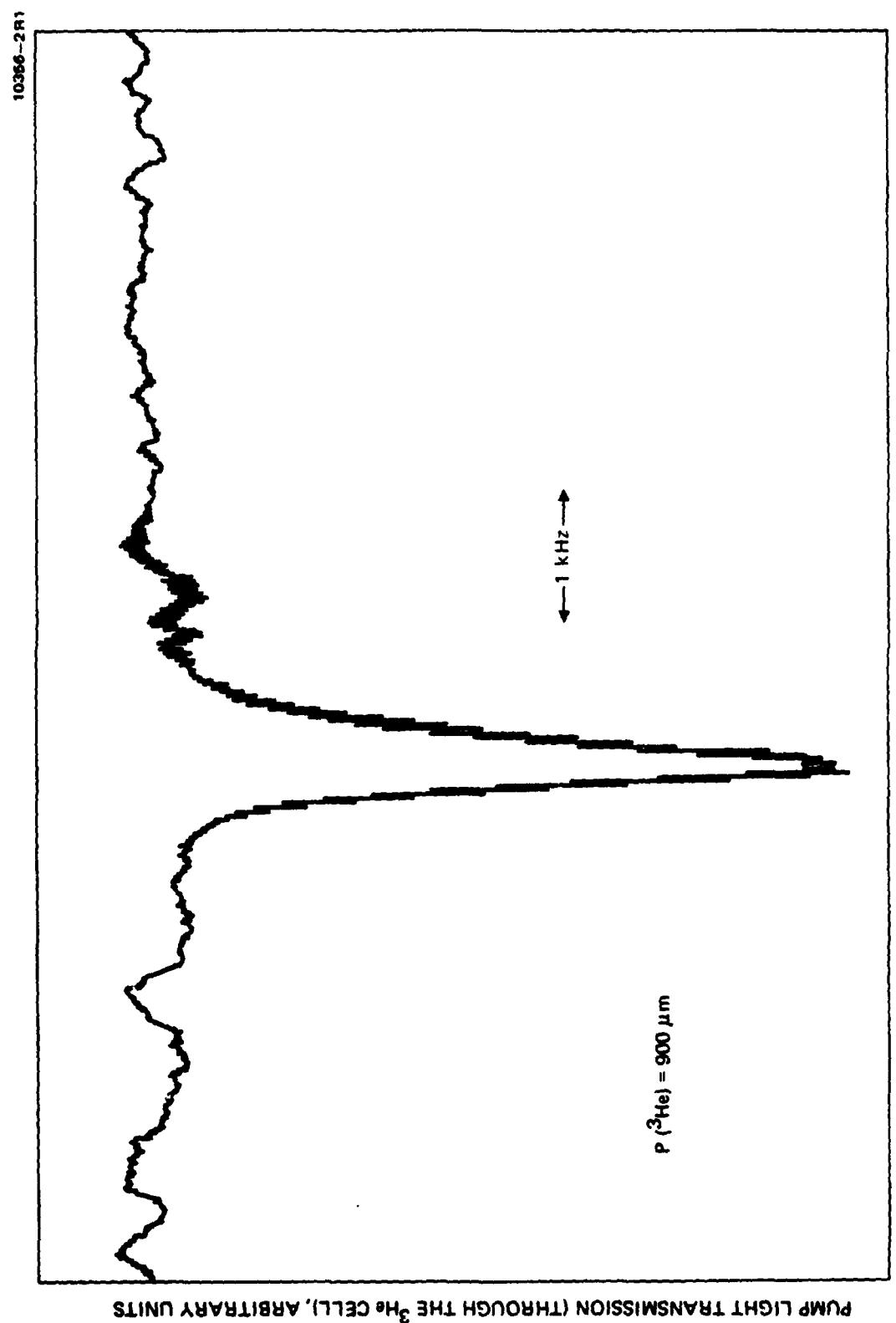
Figure 13. Ground-state ^{3}He NMR signal using pulse modulation of the Larmor frequency) and synchronous detection (time constant: 1.25 sec). For this measurement, the static magnetic field was fixed; the rf frequency (applied to the Larmor coil) was varied.

42

10356—1R1
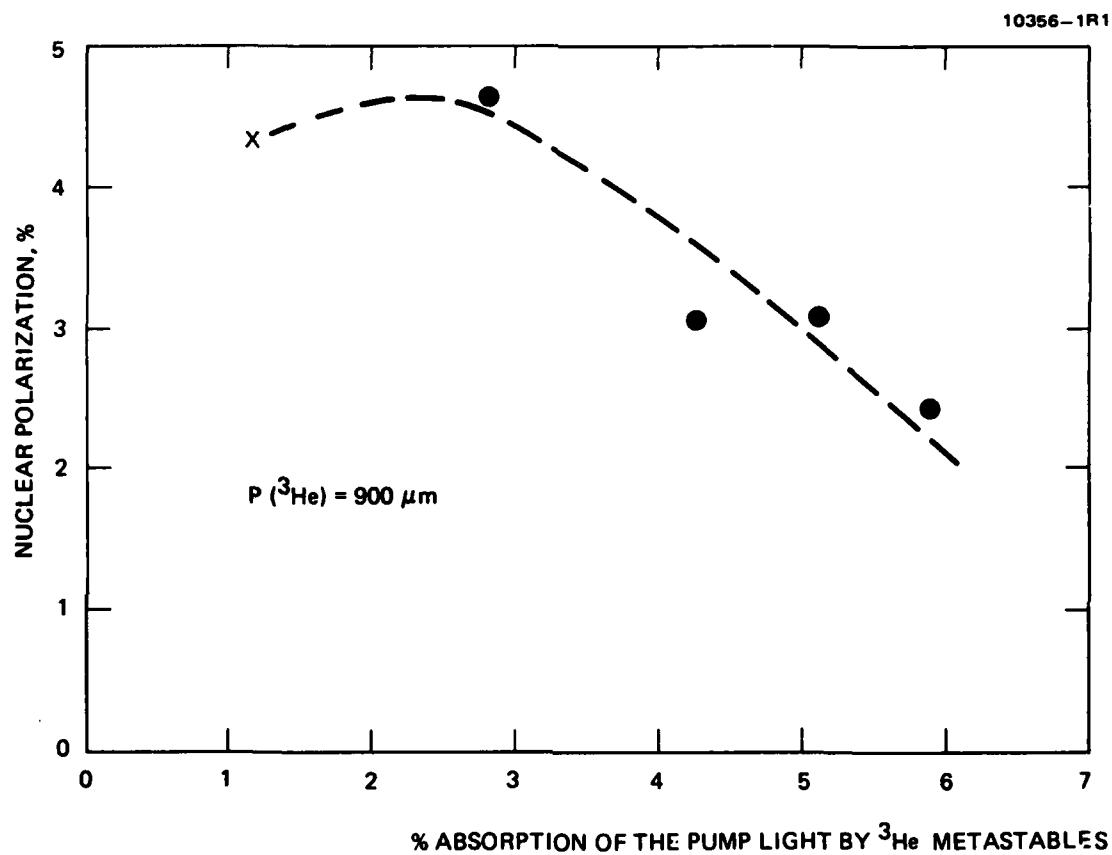
**THE DATA POINT MARKED BY AN"X"CORRESPONDS
TO THE WEAKEST, STABLE ABSORPTION CELL DISCHARGE**

Figure 14. Measured value of the nuclear polarization as a
function of metastable ^{3}He absorption of the ^{4}He
pump light (varied by changing the ^{3}He cell rf
drive power). $P(^3\text{He}) = 900$ μm. In another set
of experiments, a greater value of polarization,
9.5%, was obtained.

43

(corresponding to the F = 3/2 and F = 1/2 sublevels, respectively); and the $1\,^2S_{1/2}$ resonance of the ground ionic state of ^{3}He (^{3}He$^+$) at 1.4 MHz/g.* A typical result is shown in Figure 15. For this run, the magnetic field was scanned from ~1 to 10 G at a rate of ~1 G/min. The lock-in integration time was 4 sec. To calibrate the magnetic field, the ground-state neutral ^{3}He Larmor resonance coil was driven by a square wave. The presence of the resultant odd harmonics made coupling to the $1\,^1S_0$ nuclear resonance possible as the magnetic field (H) was swept through its range (i.e., at H_0, $3H_0$, $5H_0$, etc.). In addition to the three signals (corresponding to the ground-state resonance), both of the $2\,^3S_1$ resonances are seen. The increased width of the latter resonances is due to the smaller metastable helium (^{3}He*) lifetime which is dominated by metastability exchange collisions. The widths of the resonances cannot be precisely determined from these data. For determination it is necessary to take into account the magnetic field scan rate and detection system integration time.

(2) <u>Optical Polarization Asymmetry Technique</u> — The use of the optical polarization asymmetry (OPA) technique for the detection of magnetic resonance is important in that it can yield a higher S/N ratio.

For the results given here, we used cells containing 100 and 900 μm of ^{3}He. A typical experimental run is shown in Figure 16. For this run, the static field was slowly swept, with the simultaneous application of rf to the ground state and the metastable Larmor coils; again, a square wave was applied to the former coil for field calibration purposes. For this measurement, a cell filled to 100 μm of ^{3}He was used. In the scan we were able to identify the $1\,^2S_{1/2}$ resonance of ^{3}He$^+$. The lower fill pressure

---

*The Larmor coil frequencies were chosen so that the various resonances could be observed over our magnetic field sweep range
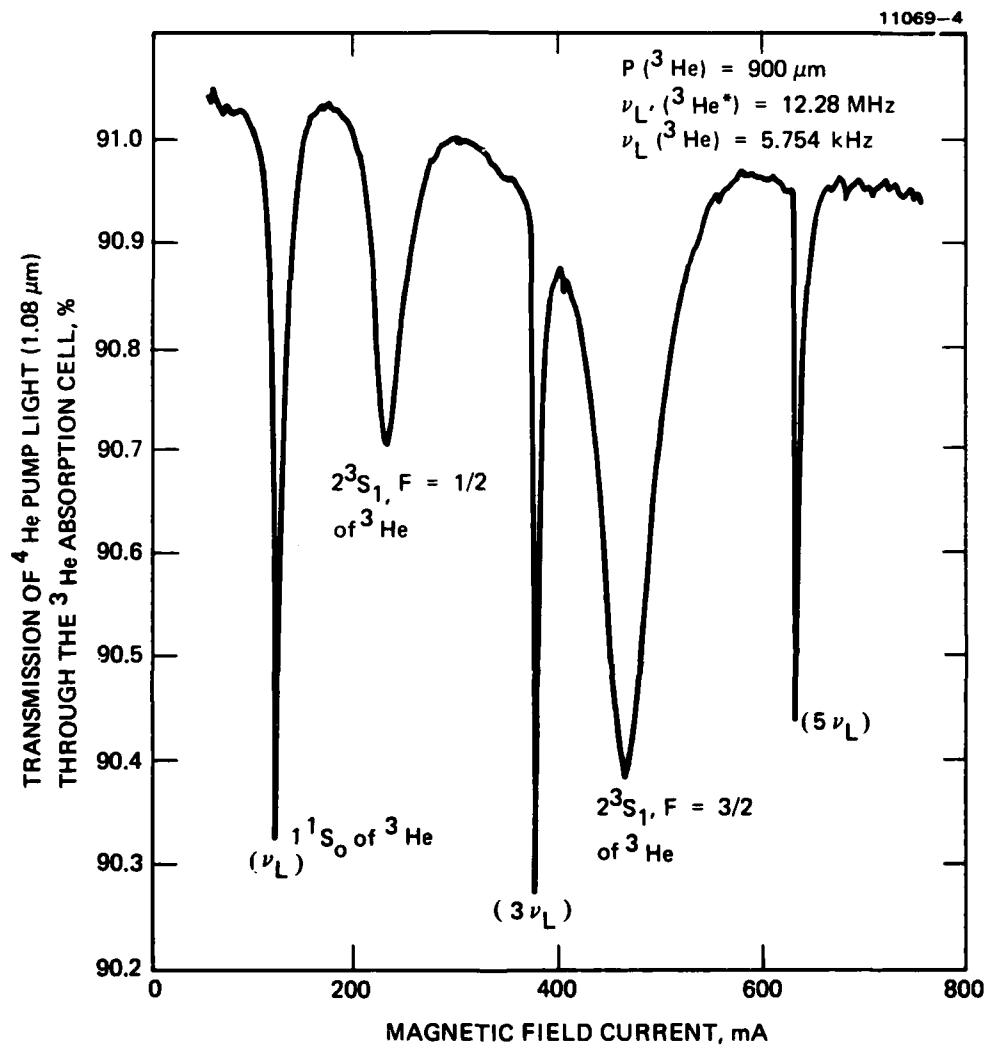
Figure 15. Observation of ^{3}He (ground state and metastable) resonances by scanning the applied magnetic field and monitoring the pump light transmission (apparatus shown in Figure 8).

45
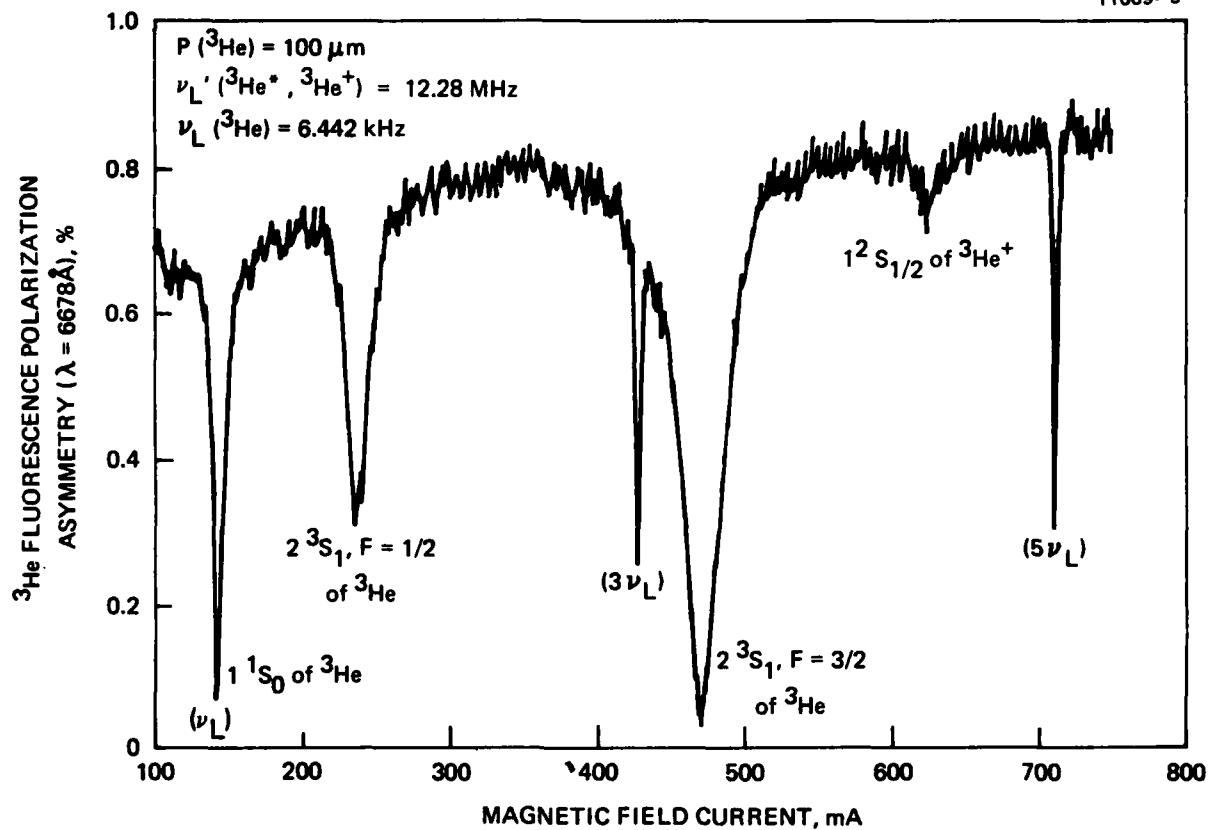
Figure 16. Observation of ^{3}He (ground state, metastable, and ground state ionic) resonances by scanning the applied magnetic field using the OPA technique (apparatus shown in Figure 10).

results in a smaller charge exchange collision rate, giving a longer ^{3}He$^+$ lifetime, and thereby increasing the S/N ratio. The observation of the ^{3}He$^+$ resonance indicates of the sensitivity of the OPA technique.

The ground-state nuclear polarization at this lower pressure (100 μm) was measured (using the pump light intensity technique) to be 3.6% as compared with a value of 9.5% for a 900 μm ^{3}He fill pressure. The value of the optical polarization asymmetry (at 6,678 Å) was measured to be ~10^{-3}, indicating a ~10% "efficiency" for the collisional transfer of the ground-state polarization to the higher lying states of helium. This is considered to be a reasonable value.
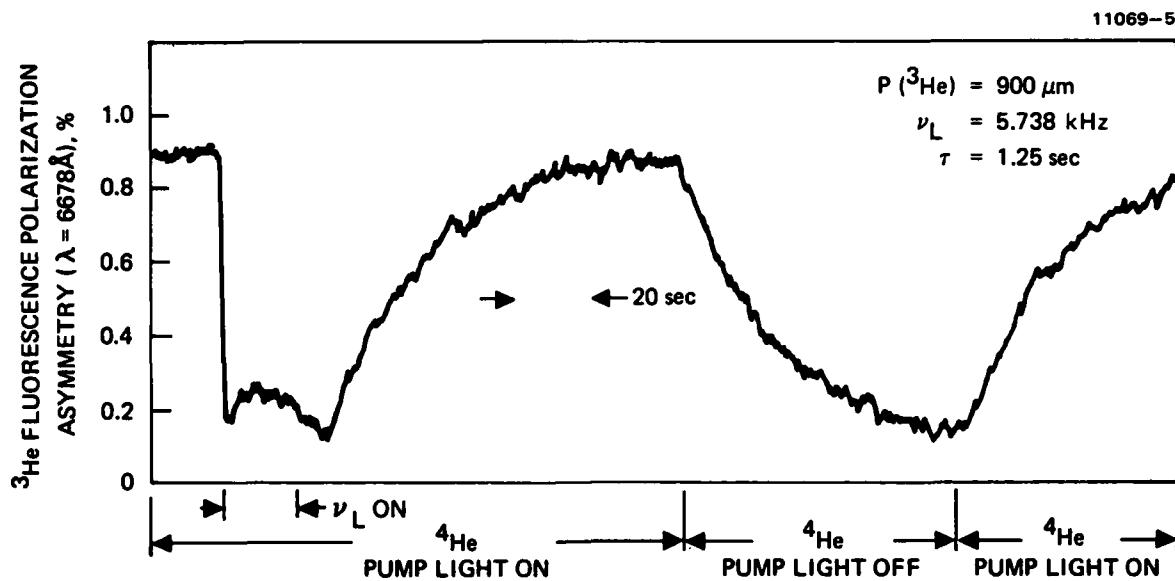
Figure 17. Decay of the OPA signal when the pump lamp radiation
is prevented from incidence upon the absorption cell.
The long decay time provided evidence of "storage"
of polarized ground state ^{3}He atoms in the ballast
region of the absorption cell.

Finally, using the OPA technique, we have observed evidence
of the "storage" of polarized ground state ^{3}He atoms in the
ballast/reservoir region of the absorption cell. This was
inferred from the long decay time (~40 to 60 sec) of the OPA
signal when the 1.08 μm ^{4}He pump light was prevented from reach-
ing the absorption cell. A typical result is shown in Figure 17.
To establish a reference, rf at the Lamor frequency was first
applied to an optically pumped ^{3}He cell thus destroying the
nuclear polarization. The OPA signal drops instantaneously to a
level reflecting random nuclear spin orientation. After the rf
was removed, the OPA signal builds up (in ~60 sec) as the ^{3}He
atoms again become optically pumped. At this point, the ^{4}He pump

47

light is blocked. The long OPA decay is now clearly seen. (The OPA signal builds up once again as the pump light is unblocked). We interpret this long decay time as follows: During the optical pumping cycle, polarized ^{3}He ($1\,^1S_0$) atoms diffuse through the capillary tube and reside (intact) within the ballast/reservoir region of the cell. After the pump light is blocked, some of these polarized atoms diffuse back into the discharge region and transfer part (~10%) of their polarization to the higher-lying ^{3}He states by collision.

We have also checked that absorption cells without ballast regions yielded short OPA decay times (~1 to 2 sec) as expected. (We note that these measurements were possible through the use of the OPA technique; the pump light transmission scheme obviously could not be used in this case.) This is an important result in that it experimentally verifies the polarization storage mechanism which is necessary for realization of the dumbbell-geometry NMR gyro sensor.

(3) **RF Impedance/Opto-Galvanic Spectroscopy** — We have observed evidence of an rf optogalvanic effect (OGE) response from our system.[15,16] The geometry used to observe this effect is shown in Figure 18. The OGE basically involves monitoring impedance changes in a discharge as a result of an external optical perturbation: the absorption of resonance radiation. Simply stated, the absorption of photons by atoms in a discharge modifies the power necessary to drive the (dc or rf) discharge. The fractional change in the lamp impedance scales roughly as the ratio of the total optical power absorbed by the discharge [P_{ABS} = $P_{PUMP}\,\alpha$ (^{3}He), where P_{PUMP} is the 1.08 μm optical pump power and $\alpha(^3$He) is the fractional absorption of the pump light by the ^{3}He metastables] to the total rf power that drives the ^{3}He (weak) discharge. We observed such effects by synchronously detecting changes in the SWR (or reflected rf power) of the ^{3}He discharge

11069-2
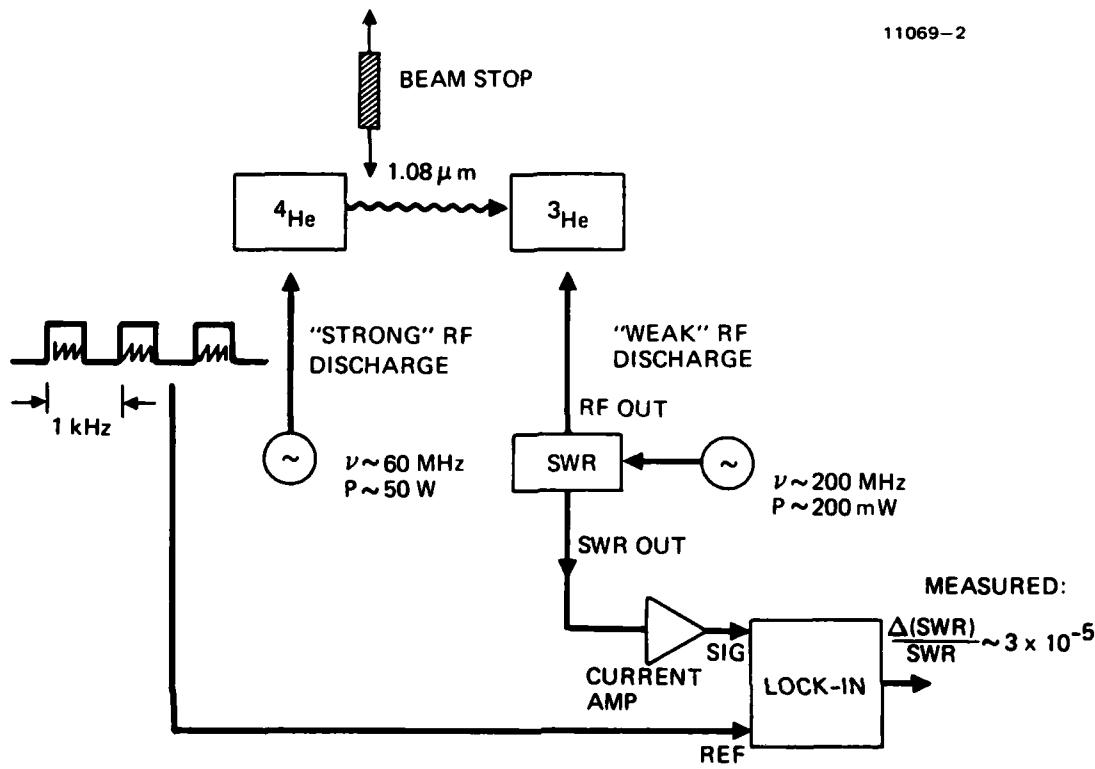
$$OGE \sim \frac{[1.08\ \mu m\ (^4He)\ POWER] \times [\alpha\ (^3He)]}{[^3He\ RF\ DRIVE]}$$

$$\simeq \frac{1/2\ mW \times 3\%\ (ABS)}{200\ mW} \sim 7 \times 10^{-5}$$

Figure 18.   Experimental apparatus used for the observation of the rf optogalvanic effect response of ^{3}He. Upon absorption of the ^{4}He pump photons (at 1.08 µm), the SWR of the ^{3}He rf drive changes, which is synchronously detected.

49

load as a result of the absorption of ^{4}He pump light. The measured value (~3 x 10^{-5}) is in reasonable agreement with a simple energy balance calculation (~7 x 10^{-5}). The significance of this phenomenon is that it has the potential to act as a reference for frequency stabilization of an optical pumping source in experiments employing nonresonant sources such as color center lasers or diode lasers. These sources were recently used either to optically pump[17] or to probe[18] the $2\,^3S_1$ state of He at 1.08 μm. This portion of the program was supported by IR&D funds.

Since the beginning of this program, other workers have independently observed effects that we proposed, including observation of an rf optogalvanic effect,[19] the use of the OGE to indicate the optical pumping of an atom[20] (the $^3P_2$ state of neon), and the stabilization of a diode laser to an atomic resonance line[21] (an AlGaAs laser, frequency locked to the D-line of Cs).

b. Heavy Noble Gases: Xe and Ne

We have successfully observed $^3P_2$ metastable state absorption and polarization through the optical pumping of various isotopes of xenon and neon. The measured values for the polarization in the isotopically enriched odd-mass-numbered isotopes studied here are comparable to values measured by other workers using naturally abundant (primarily even isotope) samples. We have also observed a factor of two increase in the polarization of ^{21}Ne when using a ^{21}Ne filled pump lamp, as compared to a lamp containing naturally abundant neon (primarily ^{20}Ne). Since the basic approach and techniques are similar for the heavy noble gases, we discuss both sets (Xe and Ne) of results in this section.

(1) Xenon — Optical pumping of xenon metastable atoms was observed using the basic experimental apparatus discussed in Section 2-C, above, and shown in Figures 3 and 8. The Pyrex pump lamp contained 6 Torr of research grade naturally abundant xenon.

50

Using an electrodeless rf discharge (60 MHz at ~50 W), ~1/3 mW of usable output at 8,819 Å was measured. The resonant radiation was made circularly polarized with a measured circularity of ~97.5%. The absorption cell contained 10 μm of 60% enriched ^{129}Xe and 50 μm of 99.99% enriched ^{3}He, which served as a buffer gas. Using a silicon photodiode and a 8,819 Å narrow bandpass filter, we measured a 25% absorption of the pump light by xenon $^3P_2$ metastable atoms in the absorption cell. The xenon metastables were produced by a weak rf electrodeless discharge.

Optical pumping of metastable $^3P_2$ xenon atoms was observed by monitoring the pump light transmission. Changes in the metastable absorption are detected as an applied dc magnetic field is slowly swept through the Zeeman resonances in the presence of a 12 MHz rf test signal applied in a direction perpendicular to the quantization axis.

Figure 19 shows results of a typical experimental run, where the relative transmission of the 8,819 Å pump light through the absorption cell is plotted as a function of the dc solenoid current. For this measurement, the 12 MHz test signal was amplitude modulated at 18 Hz. The silicon photodiode output was synchronously detected using a lock-in amplifier with a time constant of 4 sec. As shown in the figure, six resonances corresponding to the xenon isotopes ^{129,131,132}Xe are clearly visible. In addition to the strong resonance of the even isotope, ^{132}Xe, resonances corresponding to the $\Delta F = 0, \Delta m_F = 1$ hyperfine Zeeman transitions of the odd mass-numbered xenon isotopes can also be identified. The various resonances were identified using the Landau g-factor values. The transmission amplitude changes observed yield a metastable polarization of ~2 x 10^{-3}, in agreement with the values reported in the literature.[13]

We note that neither the ^{129}Xe nor the ^{3}He ground-state nuclear resonances were observed. The absence of the xenon

51
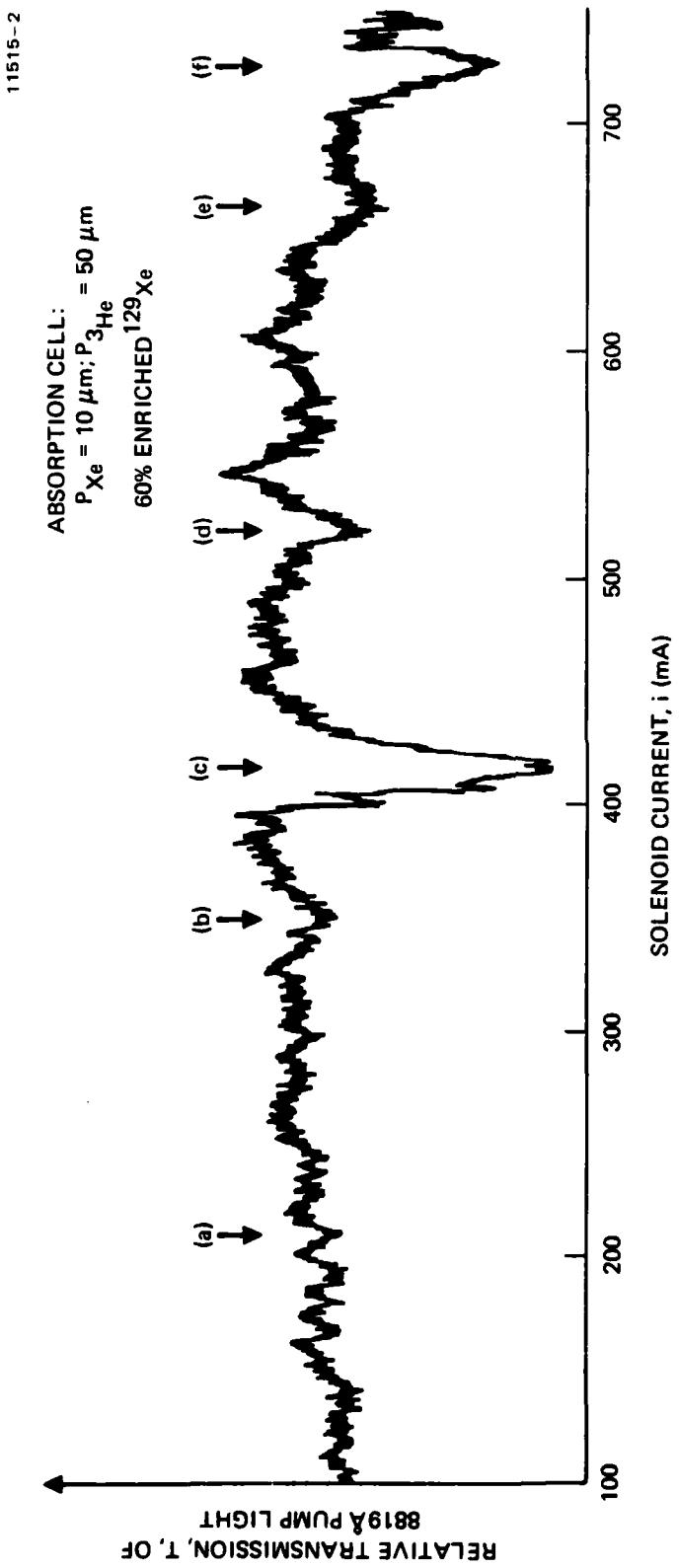
Figure 19. Optical pumping of $^3P_2$ Xe metastables synchronously detected by amplitude modulating the applied rf test signal.

resonance may be due to depolarizing collisions with even-numbered xenon isotopes (since our ^{129}Xe sample is only 60% enriched), multispectral line absorption, which results in a radiatively induced polarization loss mechanism to the ground state, or the system S/N ratio. Also, since there are no resonance coincidences in the He-Xe system, the absence of angular momentum transfer during collisions is not unexpected, which is confirmed by the absence of the ^{3}He resonance.

To improve the S/N ratio, a closed-packed geometry was configured, with the pump lamp placed adjacent to the absorption cell, resulting in an increased pump lamp flux. Also, instead of modulating the test signal, the applied magnetic field was modulated by superimposing a small ac current on the dc solenoid supply. This field modulating frequency (18 Hz) also serves as the reference in the synchronous detection of transmission changes of the pump light through the absorption cell. This magnetic field-dithering technique circumvents certain absorption cell systematic effects caused by rf field modulation. Figure 20 shows a plot of the various resonances observed using the closed-packed geometry and dithering system approach. Although the metastable resonances are clearly seen (except for the first, weak resonance), no appreciable improvement in the S/N ratio was noted.

In another attempt to observe the xenon ground-state resonance, we utilized both monochromatic optical pumping at 8,819 Å (using a narrow bandpass dielectric filter), and the optical polarization asymmetry (OPA) detection technique. The OPA scheme involves synchronously detecting changes in the optical polarization state of an isolated absorption cell fluorescence line (at 4,671 Å in the case of xenon) as the magnetic field is slowly swept through the Zeeman resonances. Again, neither of these approaches revealed ground-state polarization signals. Hence, one can conclude that the large depolarization cross section in collisions with even mass-numbered xenon isotopes reduced any possible ground-state signals below detectable levels of our

53

ABSORPTION CELL:
$P_{Xe} = 10 \ \mu m; P_{3_{He}} = 50 \ \mu m$

60% ENRICHED ^{129}Xe
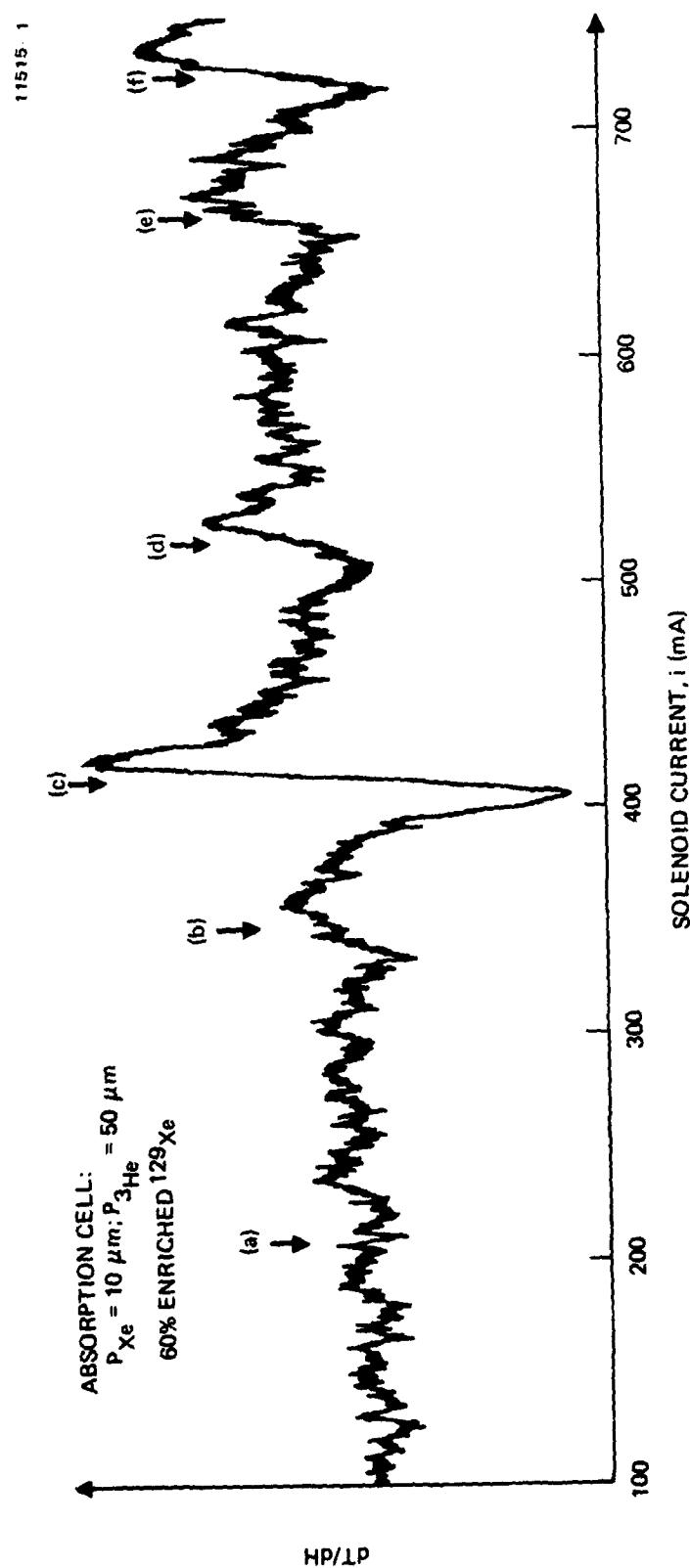
(a) ^{131}Xe; F = 1/2
(b) ^{129}Xe; F = 3/2
(c) ^{132}Xe; J = 2
(d) ^{131}Xe; F = 3/2 AND ^{129}Xe; F = 5/2
(e) ^{131}Xe; F = 5/2
(f) ^{131}Xe; F = 7/2

$\nu_L = 12.28$ MHz
$\tau_{LOCK-IN} = 4$ sec
$\nu_{REF} = 18$ Hz
SWEEP RATE: 100 mA/100 sec

SOLENOID CURRENT, i (mA)

Figure 20. Optical pumping of $^3P_2$ Xe metastables synchronously detected by dithering the dc magnetic field.

54

apparatus. Moreover, given the S/N figure of our apparatus, the absence of an OPA signal may be caused by the small density of xenon atoms in the absorption cell. (The maximum fill pressure is limited by collisional depolarization.) These two factors account for a 10^3 decrease in the excited OPA signal relative to that in ^{3}He, which would be below the detectable levels of our system.

(2) Neon — Optical pumping of neon metastable atoms was observed using pump lamps and absorption cells described earlier. The Pyrex lamp contained 2.5 Torr of research grade, naturally abundant neon. Using an electrodeless rf discharge (14 MHz ~100 W), ~1 mW of usable output at 6,402 Å was measured. The resonant radiation was made circularly polarized with a measured circularity of >98%. For these experiments, the absorption cells contained 24 µm of either research grade naturally abundant neon or 90% enriched ^{21}Ne. These cells also contained 326 µm of 99.99% enriched ^{3}He, which served as a buffer gas. Using a EMI 9558QB photomultiplier tube and a 6,402 Å narrow bandpass filter, absorption of the Ne pump light by Ne $^3P_2$ metastable atoms (in the absorption cell) was measured from ~5% to 60%, depending on the metastable Ne density. The neon metastables were produced by a weak rf electrodeless discharge. Figure 21 shows results of the measured 6,402 Å pump light absorption as a function of the absorption cell fluorescence (at 6,402 Å). The neon metastable density is assumed to be proportional to the fluorescence level.

Optical pumping of metastable $^3P_2$ ^{20}Ne and ^{21}Ne atoms was observed by monitoring the pump light transmission. Changes in the metastable absorption are detected as an applied dc magnetic field is slowly swept through the Zeeman resonances in the presence of a 12 MHz rf test signal, which was applied in a direction perpendicular to the quantization axis.

Using the absorption cell containing naturally abundant neon (with ^{3}He as the buffer gas), the relative transmission of the 6,402 Å pump light through the absorption cell as a function of the dc solenoid current is shown in Figure 22. The time constant of the detection system is 4 sec. As shown in the figure, the

% ABSORPTION OF ^{NAT}Ne PUMP LIGHT (λ = 6402Å) THROUGH THE ^{21}Ne CELL

MAX RF OUTPUT TO ^{21}Ne CELL

WEAKEST STABLE
^{21}Ne CELL RF
DISCHARGE

$\nu \simeq 14$ MHz

$\nu \simeq 144$ MHz

6402Å FILTERS

KEITHLEY
427 i–AMP

L   PUMP
LAMP   L   ABS
CELL   L   L   SCOPE

ATTENUATOR   EMI 9558QB PMT

^{21}Ne ABSORPTION CELL FLUORESCENCE/RF DRIVE POWER, ARBITRARY UNITS
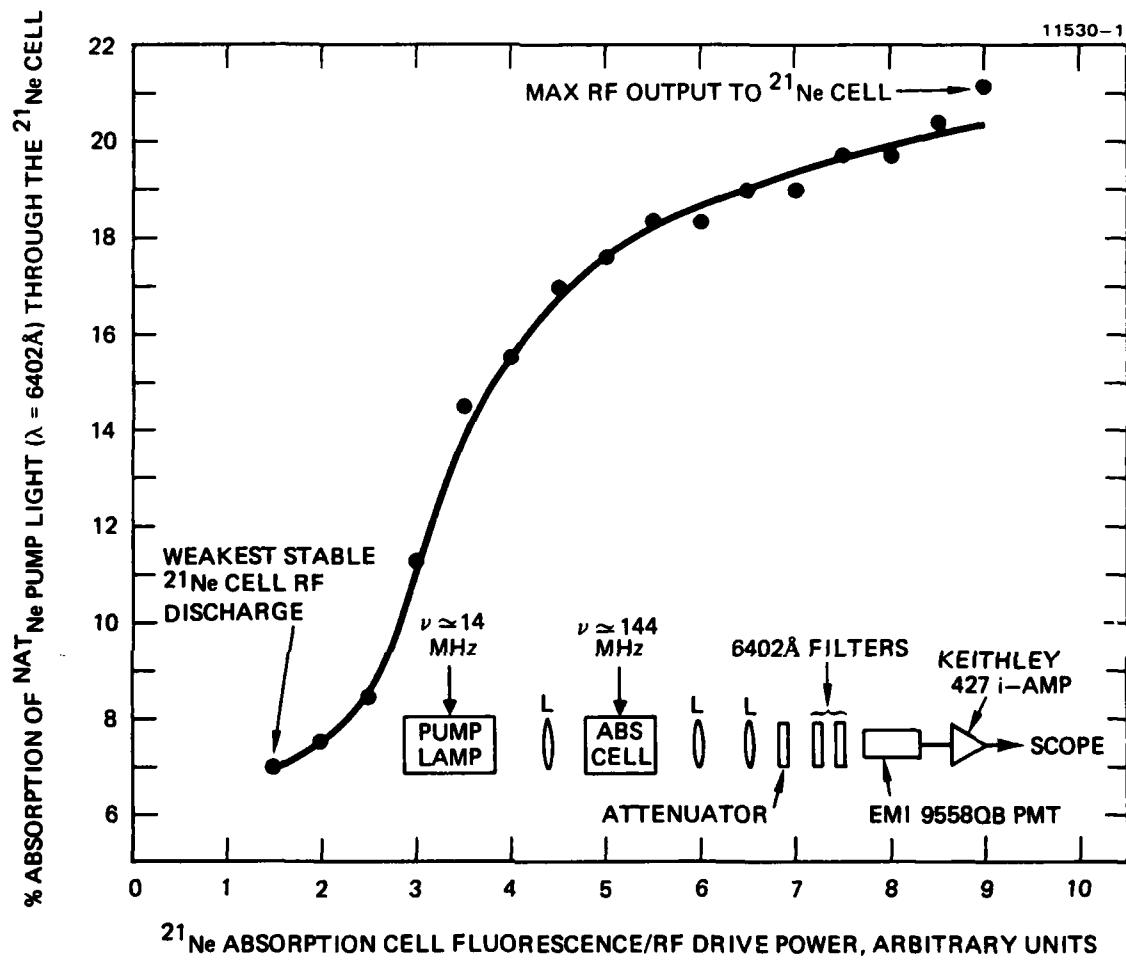
Figure 21. Observation of the absorption of pump light
(λ = 6,402 Å) by $^3P_2$ metastable neon atoms.

11515—4

PUMP LAMP:
$P(NAT_{Ne}) = 2.5$ TORR

ABSORPTION CELL:
$P(NAT_{Ne}) = 24 \mu m; P(^3He) = 326 \mu m$
2 IN. DIA x 2 IN. LONG; NO BALLAST

$\nu_L = 12.28$ MHz
$\tau_{LOCK-IN} = 4$ sec
$\nu_{REF} = 18$ Hz
SWEEP RATE = 100 mA/100 sec
FIELD CALIBRATION $\approx 1.41 \times 10^{-2}$ GAUSS/mA

(a) ^{20}Ne; J = 2; $g_J = 3/2$

Ne* ABSORPTION $\approx 54\%$

Δ(ABSORPTION)$_{MAX} \approx 2 \times 10^{-3}$

$$g_J = 1 + \frac{J(J+1) - L(L+1) + S(S+1)}{2J(J+1)}$$

$$\frac{\delta\nu}{\delta H} = g \ (1.4 \text{ MHz/GAUSS})$$

SOLENOID CURRENT, i, mA

RELATIVE TRANSMISSION, T, OF 6402Å PUMP LIGHT

(a) →
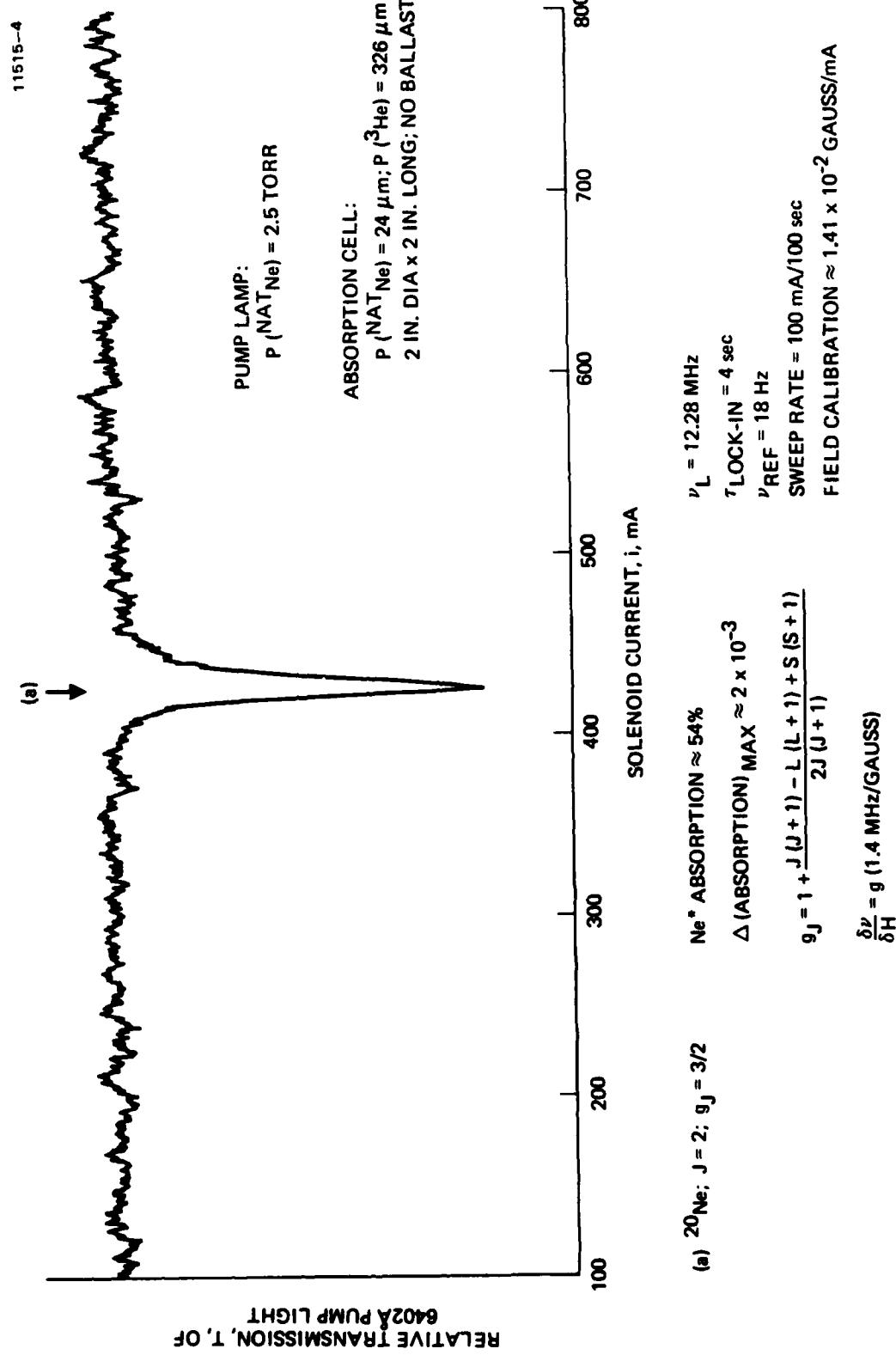
Figure 22. Optical pumping of $^3P_2$, ^{20}Ne.

57

resonance of the even isotope (^{20}Ne) has an excellent S/N ratio, although the estimated metastable polarization is only ~2 x 10^{-3}.

The results obtained using an absorption cell containing ~90% enriched ^{21}Ne, and ^{3}He as a buffer gas is shown in Figure 23. Five resonances corresponding to the neon isotopes ^{20,21}Ne are visible. In addition to the resonance of the even isotope, ^{20}Ne, resonances corresponding to the $\Delta F = 0$, $\Delta m_F = 1$ hyperfine Zeeman transitions of the $^{3}P_2$ metastable ^{21}Ne isotope can be seen. The various resonances were identified by their relative Landau g-factor values. We note that the ^{21}Ne ground-state resonance was not observed. We attribute this result to a low value for the observed neon metastable state polarization. We further note that the OPA approach (using the neon fluorescence line at 5,400 Å) did not reveal a detectable signal, for reasons similar to the xenon case.

Several approaches to improve the neon polarization were attempted: narrowband, filtered pump lamp emission; laser pumping, matched spectral line overlap; and collision transfer (to be discussed in the next subsection). The latter two techniques resulted in an improvement of the polarization by factors of two and five, respectively (relative to the above results).

The use of filtered pump light emission (at 6,402 Å) did not result in a detectable neon signal, primarily because of the drastic decrease in flux throughput (as a result of the line-center filter transmission and its narrow FOV). Using IR&D funding, we also attempted to use (unsaturated) dye laser radiation to obtain single-line optical pumping. The absence of a signal using this technique is attributed to the fact that the laser was not actively stabilized (both in frequency and amplitude). Although small frequency jitter (over the Doppler-broadened absorption line) may be of benefit in uniformly exciting all velocity groups of the absorbing atoms,[22] the large frequency excursions of our laser and mode-hopping effects severely limited the photon coupling efficiency to the atomic system. In recent spectroscopic studies of neon,[12,20] precision interferometric

PUMP LAMP:
P (^{NAT}Ne) = 2.5 TORR

ABSORPTION CELL:
90% ENRICHED ^{21}Ne (I = 3/2)
P (^{21}Ne) = 24 μm; P (^{3}He) = 326 μm
2 IN. DIA × 2 IN. LONG; NO BALLAST

(a)　(b)　(c)　(d)　(e)

SOLENOID CURRENT, i, mA

100　200　300　400　500　600　700　800

RELATIVE TRANSMISSION, T, OF 6402Å PUMP LIGHT

(a) ^{21}Ne; F = 1/2; g_F = 3
(b) ^{20}Ne; J = 2; g_J = 3/2 = 1.5
(c) ^{21}Ne; F = 3/2; g_F = 6/5 = 1.2
(d) ^{21}Ne; F = 5/2; g_F = 33/35 = 0.94
(e) ^{21}Ne; F = 7/2; g_F = 6/7 = 0.86

Ne* ABSORPTION ≈ 50%

Δ (ABSORPTION)$_{MAX}$ ≈ 5 × 10^{-4}

$$g_J = 1 + \frac{J(J+1) - L(L+1) + S(S+1)}{2J(J+1)}$$

$$g_F \approx g_J \frac{F(F+1) + J(J+1) - I(I+1)}{2F(F+1)}$$

$$\frac{\delta \nu}{\delta H} = g \text{ (1.4 MHz/GAUSS)}$$

ν_L = 12.28 MHz

$\tau_{LOCK-IN}$ = 4 sec

ν_{REF} ≈ 18 Hz

SWEEP RATE = 100 mA/100 sec

FIELD CALIBRATION ≈ 1.41 × 10^{-2} GAUSS/mA

Figure 23.　Optical pumping of $^3P_2$ ^{20}, ^{21}Ne metastable atoms using a NATNe filled pump lamp.

stabilization techniques were required. The use of the
optogalvanic effect, with proper servo techniques, may be useful
in minimizing the frequency jitter of the dye laser. In addi-
tion, the amplitude fluctuations of our laser were far greater
than the metastable resonance induced transmission changes.
As discussed in the case of helium, the pump light fluctuations
can affect the optical pumping process.[14]

In another series of experiments, we conducted a comparison
of ^{21}Ne versus ^{NAT}Ne as the pump lamp species for the direct
optical pumping of low pressure (~24 µm) ^{21}Ne. It was observed
that, when using ^{21}Ne as the pump source, the metastable polari-
zation of ^{21}Ne was a factor of two greater than that using ^{NAT}Ne
filled pump lamps. Figure 24 shows a typical spectrum of
^{3}P$_2$ metastable resonances using this approach. (The weak yet
resolvable and reproducible resonance near the F = 3/2 line,
which corresponds to a Landau g-factor of 1.25 has not been iden-
tified.) The improved S/N in the present case is clearly evident
when compared with that using a ^{NAT}Ne pump lamp (Figure 23).
We attribute this improvement to a "matched" overlap of the pump
lamp emission lines with the absorption cell absorption profiles.
This result is consistent with that reported in studies[1] involv-
ing optical pumping of ^{3}He: in the low-pressure regime (where
collisional-induced mixing is not significant), the use of a
matched system (^{3}He for both pump lamp and absorption cells) gave
rise to greater polarization than did the use of a ^{4}He pump
lamp.

11515—3R1

PUMP LAMP:
90 % ENRICHED ^{21}Ne
P (^{21}Ne) = 2 Torr

ABSORPTION CELL:
90% ENRICHED ^{21}Ne (I = 3/2)
P (^{21}Ne) = 24 μm
2 in. DIA x 2 in. LONG, NO BALLAST

RELATIVE TRANSMISSION, T, OF 6402 Å PUMP LIGHT

(a)   (b)   (c)   (d)   (e)

$\nu_L \sim$ 12 MHz

P $\lambda/4$ 6402 Å

^{21}Ne ^{21}Ne

SOLENOID CURRENT, I, mA

(a) ^{21}Ne; F = 1/2, g_F = 3

(b) ^{20}Ne; J = 2; g_J = 3/2 = 1.5

(c) ^{21}Ne; F = 3/2; g_F = 6/5 = 1.2

(d) ^{21}Ne; F = 5/2; g_F = 33/35 = 0.94

(e) ^{21}Ne; F = 7/2; g_F = 6/7 = 0.86

Ne* ABSORPTION $\approx$ 50 %

Δ (ABSORPTION)$_{MAX}$ $\approx 2 \times 10^{-3}$

$g_J = 1 + \dfrac{J(J+1) - L(L+1) + S(S+1)}{2J(J+1)}$

$g_F \approx g_J \dfrac{F(F+1) + J(J+1) - I(I+1)}{2F(F+1)}$

$\dfrac{\delta \nu}{\delta H} = g$ (1.4 MHz/GAUSS)

$\nu_L \sim$ 12 MHz

$\tau_{LOCK-IN}$ = 4 sec

ν_{REF} = 18 Hz

SWEEP RATE = 100 mA/ 100 sec

FIELD CALIBRATION $\approx 1.41 \times 10^{-2}$ GAUSS/mA

Figure 24. Optical pumping of $^3P_2$ ^{20,21}Ne metastable atoms using a ^{21}Ne filled pump lamp.

61

2. Optical Pumping of Binary Noble Gas Mixtures

In this section, we discuss experimental results that may provide a solution to the realization of an all-noble-gas, dual-isotope, low-cost, compact NMRG sensor. Since performance of the sensor is directly proportional to the S/N ratios of the resonant transitions employed, significant polarization in both isotopic species that comprise the sensor is a critical requirement. Moreover, for a low-cost, compact geometry, a single optical pumping source that can simultaneously polarize both working species is desirable. Finally, narrow linewidths are essential to yield the required system performance. The successful experimental results to be discussed in this section appear to present a solution to these constraints.

We have observed collision-induced polarizaton transfer from optically pumped helium to excited states of neon (as discussed in Section 2-B and sketched in Figure 6). The 2^3S_1 helium metastable state, being in close energy coincidence with the $2p^54s$ manifold of neon, when optically pumped (at 1.08 μm), can transfer polarization to the neon atom. By cascade optical transitions, part of this polarization is preserved, being transferred to lower-lying neon levels. When the polarization of an absorption cell neon spectral line is monitored, the polarization of the upper level (of the fluorescence line) becomes apparent. The presence of optical polarization here indicates the transfer of angular momentum from the directly pumped species (He) to the "buffer" gas (Ne).

In this study, (direct) optical pumping of helium was accomplished using a ^{4}He pump lamp, with the servoloop control system (described in Section C-2 and shown in Figure 9). The emission at 1.08 μm was made circularly polarized, irradiating an absorption cell containing a mixture of helium (at 300 μm) and neon (at 5 μm). For these measurements, four cells were used containing various isotopes of both species: ^{4}He-^{20}Ne, ^{4}He-^{21}Ne, ^{3}He-^{20}Ne, and ^{3}He-^{21}Ne. The mechanism of polarization transfer from helium to neon was experimentally established by synchronously detecting the OPA signal of the absorption cell

62

fluorescence line of neon at 6,402 Å along the quantization axis. Figures 25 through 28 show experimental results for the respective absorption cells.* In all four cases, the OPA signal decreases (i.e., the neon fluorescence becomes isotropic) whenever the "source" of polarization (helium) is depolarized. The OPA signal also vanishes when the ^{4}He pump lamp is extinguished. In Figures 25 and 26, cells containing mixtures of ^{4}He-^{20}Ne and ^{4}He-^{21}Ne were tested. In both cases, where ^{4}He is the optically pumped species, the Zeeman resonance of the ^{4}He metastable state (2^3S_1) is clearly seen. The magnitude of the signal (~1%), coupled with the excellent S/N ratio, provide evidence that the upper level of the 6,402 Å transition (the $^3D_3$ state) is strongly polarized, as is the ^{4}He 2^3S, state.

The similarity of Figures 25 and 26, in terms of S/N ratio and magnitude, indicates that the resultant $^3D_3$ Ne polarization is comparable for both ^{20}Ne and ^{21}Ne (despite the more complex hyperfine spectrum of ^{21}Ne). This same result is evident by comparing Figures 27 and 28, where cells containing mixtures of ^{3}He-^{20}Ne and ^{3}He-^{21}Ne were used. In this set of experimental runs, ^{3}He is the optically pumped species. The resultant ^{3}He spectrum, showing the 1^1S_0 ^{3}He ground state and associated odd harmonics of the Larmor signal, along with the two 2^3S_1 metastable resonances, again indicates that the polarization transfer mechanism is comparable using either odd or even neon isotopes.

Unfortunately, in this study, the OPA detection technique is insensitive to the ground and the metastable neon Zeeman resonances. The reason for this is the tight coupling of the OPA

---

*For Figures 25 through 28, the magnetic field solenoid-current sweep rate was 100 mA/100 sec, the lock-in amplifier time constant was 4 sec, and the reference frequency was 18 Hz. The cylindrical (Pyrex) pump lamps were 1 in. in diameter and 1 in. long, with a barium getter-coated reservoir filled with 2 Torr of ^{4}He.
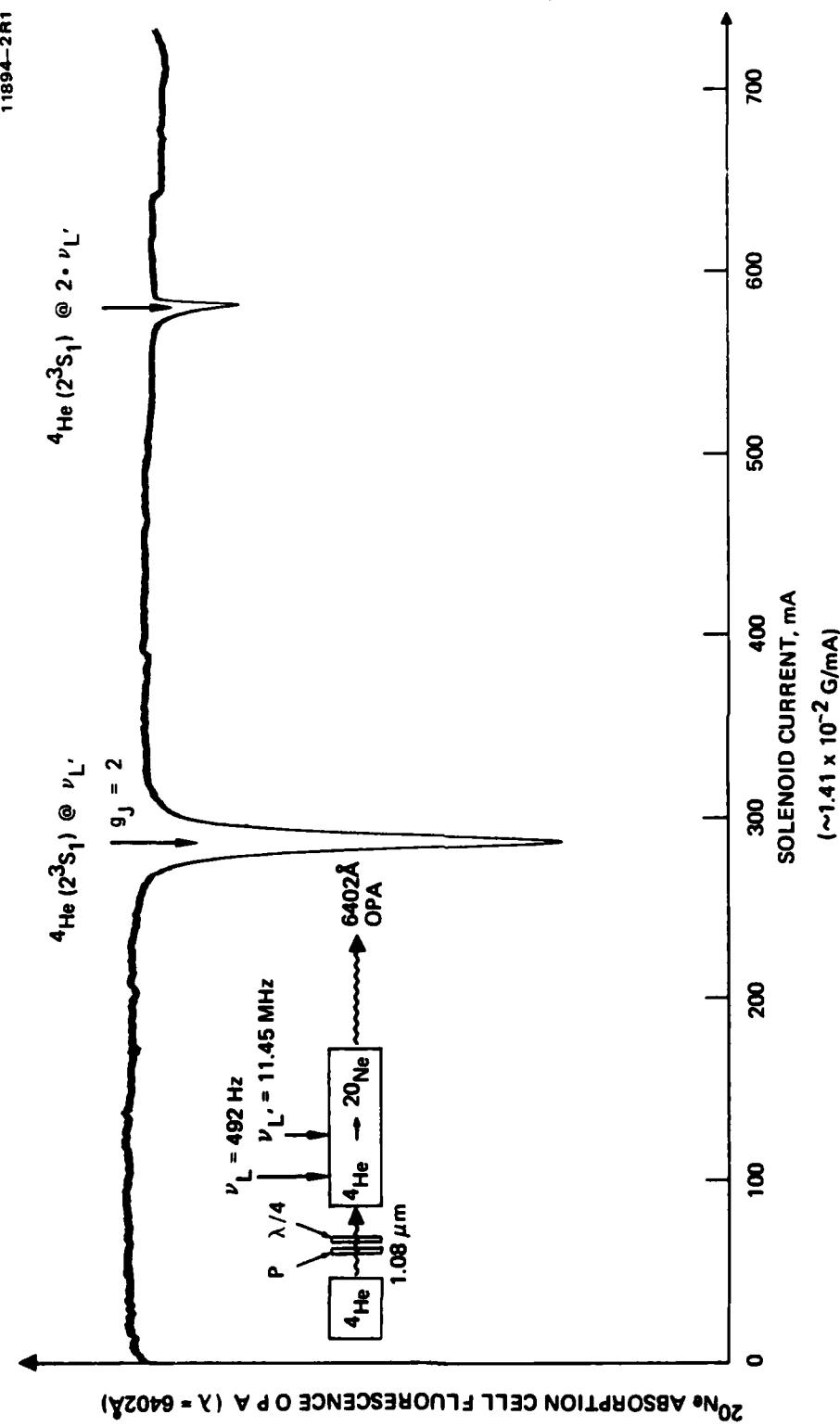
Figure 25. Polarization transfer from optically pumped ^{4}He to ^{20}Ne. Helium Zeeman resonances in a cell containing a mixture of ^{4}He and ^{20}Ne detected by observing the polarization of the 6,402 Å emission line of ^{20}Ne.

64
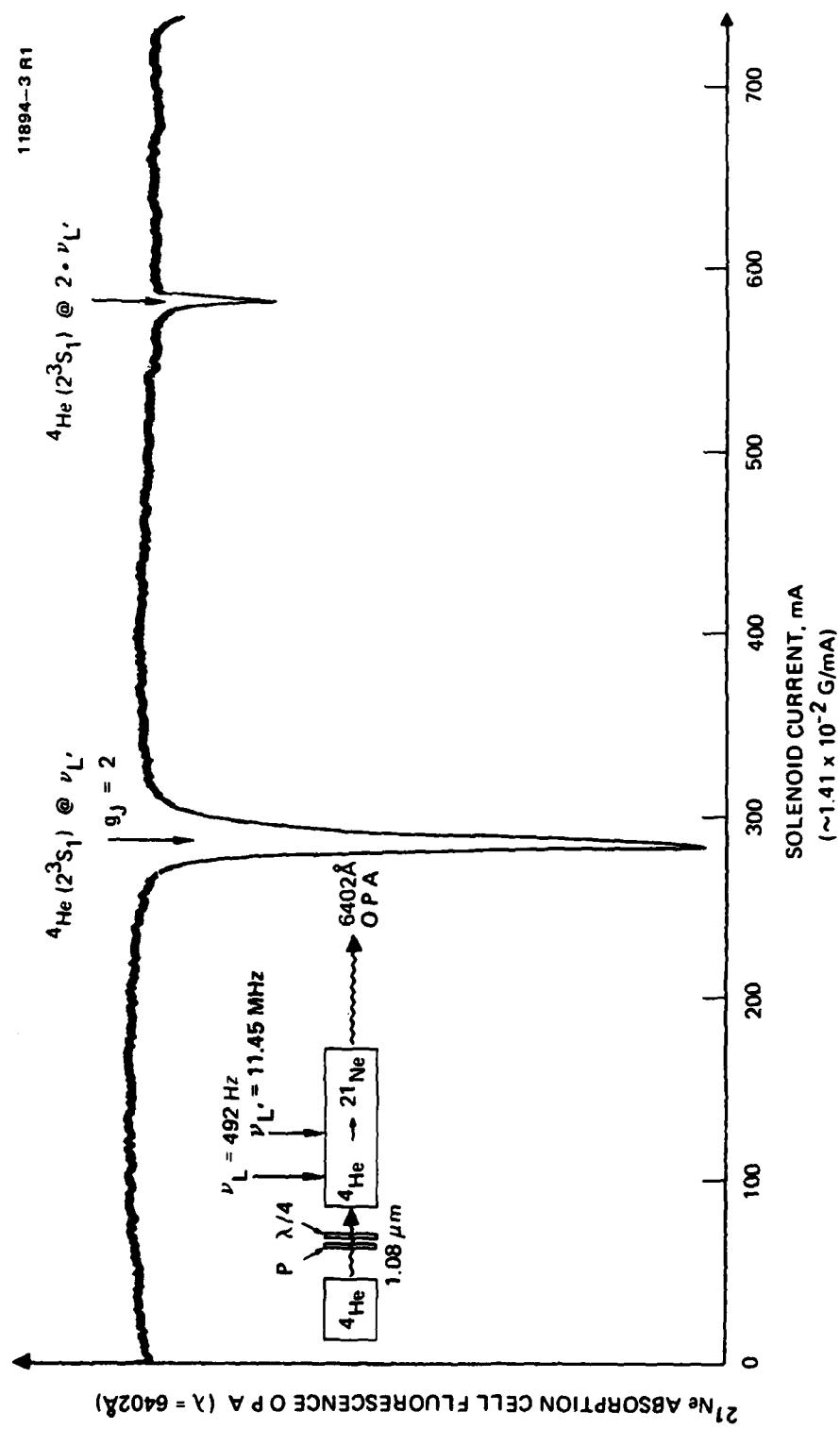
Figure 26. Polarization transfer from optically pumped ^{4}He to ^{21}Ne. Helium Zeeman resonances in a cell containing a mixture of ^{4}He and ^{21}Ne detected by observing the polarization of the 6,402 Å emission line of ^{21}Ne.
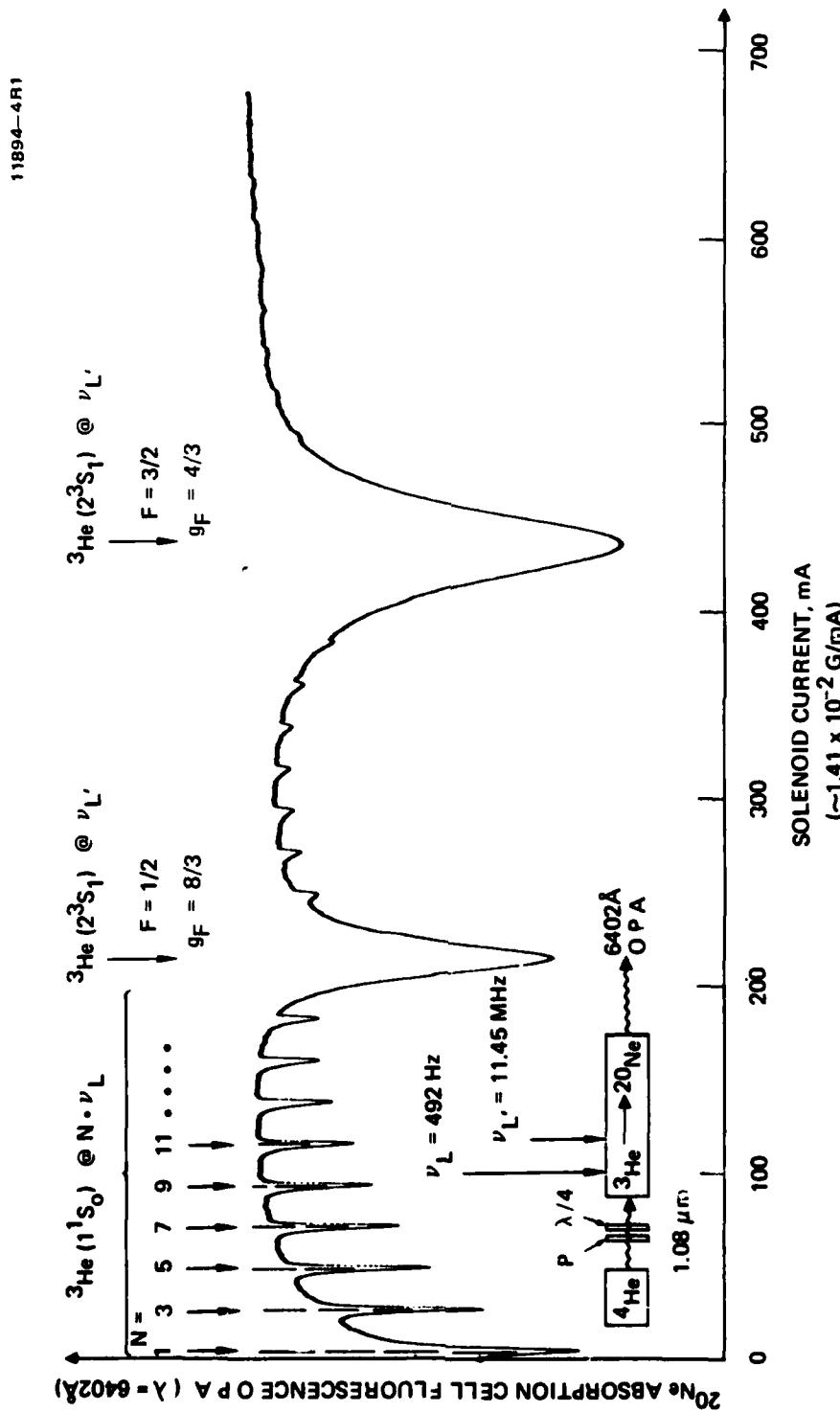
Figure 27. Polarization transfer from optically pumped ^{3}He to ^{20}Ne. Helium Zeeman resonances in a cell containing a mixture of ^{3}He and ^{20}Ne detected by observing the polarization of the 6,402 Å emission line of ^{20}Ne.
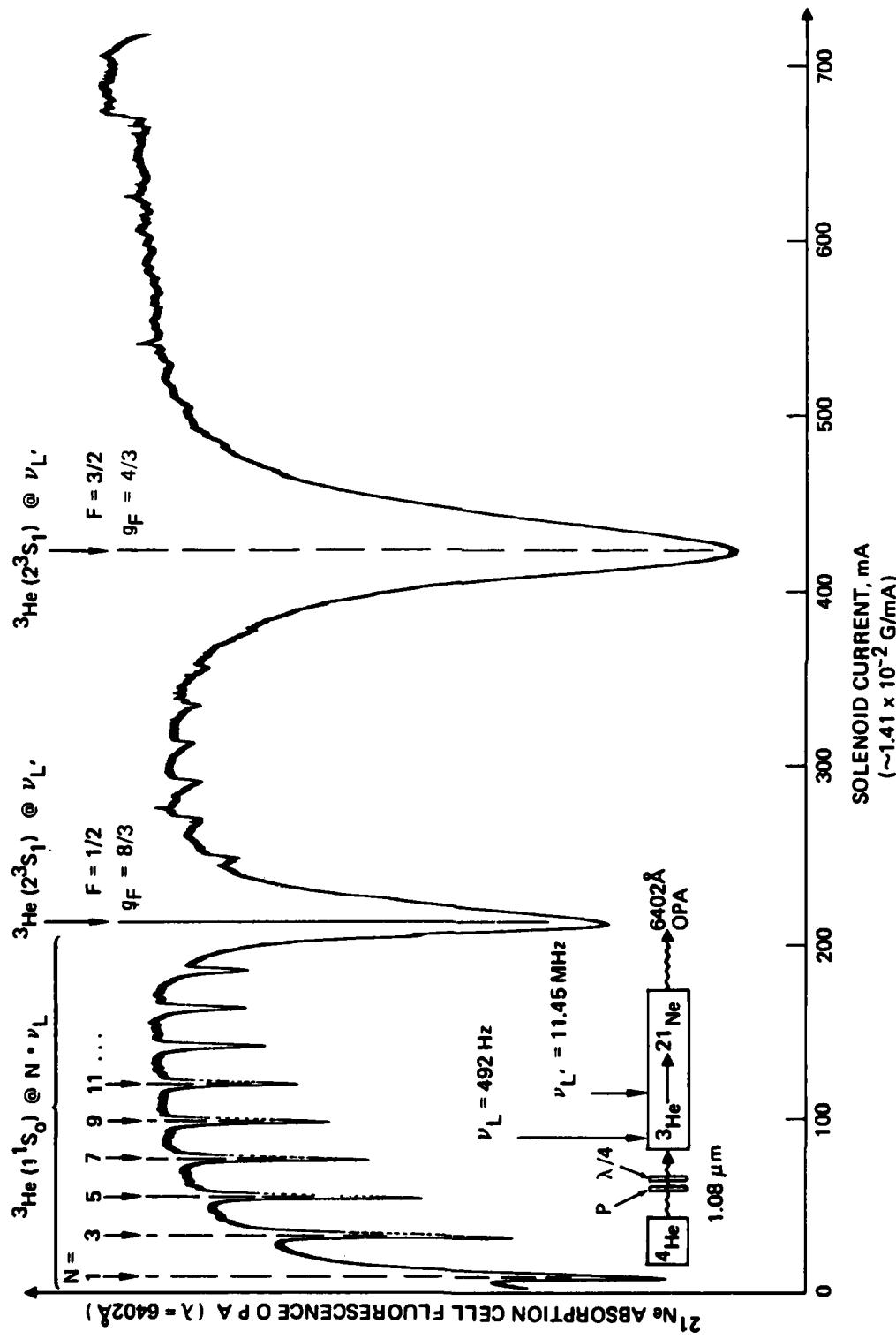
Figure 28.   Polarization transfer from optically pumped ^{3} He to ^{21} Ne. Helium Zeeman resonances in a cell containing a mixture of ^{3} He and ^{21} Ne detected by observing the polarization of the 6,402 Å emission line of ^{21} Ne.

67

signal to the source of atomic angular momentum. Thus, ground and metastable helium resonances which perturb the reservoir of **atomic angular momenta in the optical pumping cell are easily** observed, since polarization transfer from helium is to the $2p^54s$ levels of neon. The perturbation on the polarization of these and other shortlived excited states caused by ground and metastable neon resonances will be quite small, by at least the ratio of the lifetimes. However, it should be possible to observe the polarization of the neon metastable and ground states by direct rf NMR detection techniques. These observations of collisional angular momentum transfer are significant for several reasons:

- The all-gaseous ^{3}He and ^{21}Ne system can be polarized using only a single optical pumping source (at 1.08 μm). Combined with the elimination of a metallic vapor (Rb, Hg, etc.), which can lead to detrimental effcts on the gyro performance, this technique is important for practical device applications.

- The near-energy coincidence of metastable ($2\,^3S_1$) helium with the excited state ($2p^54s$) manifold of neon results in a very efficient collision-induced transfer of polarization from optically pumped He to Ne.

- This transfer mechanism is not materially degraded when using odd isotopes for one or both of the interacting species.

- The polarization of ground-state ^{3}He is not significantly degraded by the presence of neon in the system.

These results lead us to expect a reasonably large nuclear polarization in the ground state of ^{21}Ne. Thus, we expect that a pair of polarized ground-state species (^{3}He and ^{21}Ne) can be simultaneously created, using a compact, lightweight geometry. This can result in a fast warm-up, inexpensive tactical gyro sensor.

The thrust of a follow-on AFOSR-supported program is
directed toward an exhaustive study of the collision-induced
polarization mechanism, and a search for nuclear polarization of
ground-state ^{21}Ne atoms. We are considering the effect of the
collision transfer mechanism as a function of the absorption cell
fill pressure, He:Ne partial pressure, discharge conditions, and
lamp geometry. In addition, dual-cell configurations will be
evaluated in terms of the effect of the storage time (as well as
the above parametric dependencies) on the attainable S/N ratio
and the linewidth of the polarized species. The polarizations of
metastable and ground-state neon atoms will be indicated either
optically (through the use of a 6,402 Å probe beam, e.g.), or
directly, using rf NMR techniques.

The results of the investigation will enable us to make a
system analysis of the anticipated performance for a dual-
isotope, noble-gas gyro. Specific details such as the S/N ratio
and the angular rate sensitivity can be estimated. These param-
eters will greatly facilitate the evaluation of the desirability,
design parameters, and the fabrication of a breadboard gyro
sensor.

SECTION 3

CONCLUSION AND SUGGESTIONS FOR FUTURE INVESTIGATIONS

The initial objective of this program were to investigate the physics of a dual-isotope, optically pumped NMR gyro sensor. Specifically, the goal was to obtain simultaneously ground-state polarization of a binary noble-gas mixture in a dual-chamber absorption cell, and to characterize parameters such as linewidths, syste-matic frequency shifts, and broadening mechanisms. The initial thrust of this program was to construct an apparatus that would be capable of detecting polarization of the candidate species using optical techniques.

The candidate system initially proposed was a pair of odd-mass-numbered xenon isotopes, ^{129}Xe and ^{131}Xe. This pair was chosen since a single optical source could simultaneously pump both species, and because the measured ground-state lifetime is appreciable (~24 min).

As a result of this program, we determined that, after a system checkout using ^{3}He as a reference, xenon would not be suitable because of the small metastable polarizations measured (~0.1%). Also, no ground-state polarization was observed in either isotope. This observation was attributed to the large depolarization cross section of xenon, its large polarizability, and the available isotopic purity of only 60%.

On the other hand our initial results lead us to conclude that the odd isotope pair of ^{3}He and ^{21}Ne constituted a promising, if not the optimal set of species for a NMRG sensor. The large ground-state polarizations obtainable in ^{3}He due to its small depolarization cross section and the availability of extremely pure (>99.999%) samples is well established. The odd isotope of neon appears to be the next best candidate after ^{3}He for several reasons. Neon has the second lowest depolarization cross section and polarizability relative to helium, and is currently available with isotopic enrichments of 90%.

Perhaps the most promising aspect of the He-Ne combination is the ability to efficiently polarize both species with a single optical source (at 1.08 μm, a helium absorption line). This results from the near-resonance of the helium metastable level with the excited state manifold of neon. Our experimental results have confirmed that excited-state neon polarization as large as 1% is easily acheivable. Moreover, this large measured value was essentially independent of the isotopic composition of the $^{3\ 4}$He-$^{20\ 21}$Ne pair. In addition, according to the resonances observed, the ^{3}He ground state is also significantly polarized, even in the presence of the neon sample.

From these promising results, the future directions for continued efforts are well defined. We are now conducting experiments on an AFOSR follow-on contract, F49620-82-C-0095, with the goal of detecting ground-state polarization in both species employing rf NMR techniques, and using our novel dual-chamber absorption cell design. The parametric dependences of the detected resonances (as a function of fill pressures, cell geometry, discharge conditions, etc.) will enable us to predict the performance of a breadboard NMRG sensor. This evaluation will provide necessary data in developing future plans. The potential of realizing a compact, lightweight, rugged, all-gaseous, fast warm-up, and low maintenance NMRG sensor could provide a much needed addition to tactical device electronics.

REFERENCES

1. J. Brossel, Quantum Electronics III, edited by P. Grivet
   and N. Bloembergen (Columbia University Press, 1964),
   pp. 201-212; R.C. Greenhow, Phys. Rev. A 136, 660 (1964);
   R.S. Timsit and J.M. Daniels, Can. J. Phys. 49, 545 (1971).

2. J. Brossel, Fundamental and Applied Laser Physics, edited
   by M.S. Field, A. Javan, and N. Kurnit (Wiley, 1973),
   p. 769-790.

3. C.H. Volk, T.M. Kwon, J.G. Mark, Y.B. Kim, and J.C. Woo,
   Phys. Rev. Lett. 44, 136 (1980).

4. H.G. Robinson and Than Myint, Appl. Phys. Lett. 5, 116
   (1964).

5. G. Escher and P. Turowski, Z. Angew. Phys. 21, 50 (1966);
   P. Bley and P. Turowski, Z. Angew. Phys. 24, 57 (1967).

6. R.A. Zhitnikov, I.A. Kravtov, and M.P. Fradkin, Sov. Phys.
   Tech. Phys. 20, 955 (1976); ibid. 22, 377, 381, and 384
   (1977).

7. B.C. Grover, Phys. Rev. Lett. 40, 391 (1978).

8. E.J. Robinson, J. Levine, and B. Bederson, Phys. Rev. 146,
   95 (1966).

9. F. Sage, J.P. Lemoigne, and D. Lecler, Opt. Comm. 30, 332
   (1979); A. Noel, M. Leduc, and F. Laloë, CRAC 274, 77
   (1972).

10. L.D. Schearer, Phys. Lett. 27A, 544 (1968); Phys. Rev. Lett.
    180, 83 (1969).

11. J. Duppont-Roc, M. Leduc, and F. Laloë, Phys. Rev. Lett. 27,
    467 (1971).

12. M. Pinard, C.G. Aminoff, and F. Laloë, Phys. Rev. A 19, 2366
    (1979).

13. L.D. Schearer, Phys. Rev. 188, 505 (1969).

14. J.M. Daniels and R.S. Timsit, Can. J. Phys. 49, 525 and 539
    (1971).

15. R.B. Green, R.A. Keller, G.G. Lutha, R.K. Schenci, and
    J.C. Travis, Appl. Phys. Lett. 29, 727 (1976); W.B. Bridges,
    J. Opt. Soc. Am. 68, 352 (1978).

16. D.M. Pepper, IEEE J. Quantum Electron. QE-14, 971 (1978).

17. K.W. Giberson, C. Cheng, M. Onillion, F.B. Dunning, and G.K. Walters, Rev. Sci. Instrum. 53, 1789 (1982).

18. D. D. McGregor, AFOSR Contract No. F49620-78-C-0056.

19. C. Stancivlescu, R.C. Bobulescu, A. Surmeian, D. Popesov, I. Popescu, and C.B. Collins, Appl. Phys. Lett. 37, 888 (1980).

20. L. Julien and M. Pinard, J. At. Mol. Phys. 15, 2881 (1982).

21. S. Yamaguchi and M. Suzuki, Appl. Phys. Lett. 41, 597 (1982)

22. J.-C. Gay and W.B. Schneider, Z. Physik A 278, 211 (1976).